



UNIVERSIDADE D  
COIMBRA

Manuel Coelho Moura Ramos

EXPLORING DIRECTLY THE NEURAL CORRELATES  
OF FEEDBACK-RELATED REWARD SALIENCY DURING  
fMRI-BASED NEUROFEEDBACK

Dissertação no âmbito do Mestrado Integrado de Engenharia Biomédica,  
orientada pelo Professor Doutor Miguel Sá Sousa Castelo Branco  
e Professor Doutor Bruno Miguel Direito Pereira Leitão  
e apresentada ao Departamento de Física da Faculdade de Ciências e Tecnologias  
da Universidade de Coimbra.

Outubro de 2019



• U



C •

FCTUC

FACULDADE DE CIÊNCIAS  
E TECNOLOGIA

UNIVERSIDADE DE COIMBRA

Manuel Coelho Moura Ramos

**Exploring directly the neural  
correlates of feedback-related reward  
saliency during fMRI-based  
Neurofeedback**

Thesis submitted to the  
University of Coimbra for the degree of  
Masters in Biomedical Engineering

Supervisors:

Prof. Dr. Miguel Castelo-Branco (CiBIT, Faculty of Medicine, University of Coimbra)

Prof. Dr. Bruno Direito (CiBIT, Faculty of Medicine, University of Coimbra)

**Coimbra, 2019**

This work was developed in collaboration with:

Coimbra Institute for Biomedical Imaging and Translational Research,  
University of Coimbra



Institute of Nuclear Sciences Applied to Health



National Brain Imaging Network

Faculty of Medicine, University of Coimbra



Esta cópia da tese é fornecida na condição de que quem a consulta reconhece que os direitos de autor são pertença do autor da tese e que nenhuma citação ou informação obtida a partir dela pode ser publicada sem a referência apropriada.

This copy of the thesis has been supplied on condition that anyone who consults it is understood to recognize that its copyright rests with its author and that no quotation from the thesis and no information derived from it may be published without proper acknowledgement.

---

*Dedicado aos meus pais, com toda a minha gratidão*

# Agradecimentos

Queria começar por agradecer aos professores que leccionaram a disciplina de *Visão Computacional e Percepção Biológica* no ano letivo de 2017/2018, especialmente à Prof. Otilia D'Almeida encarregue do meu projeto de disciplina e ao Prof. Miguel Castelo Branco por me ter permitido "perseguir" um tema da minha escolha para Projeto de Tese.

Agradeço a todas as pessoas que me ajudaram durante o meu tempo no iCBR. Gostava de agradecer especialmente à "Scrum Team" por todos os contributos e momentos partilhados. Queria agradecer em especial ao João Pereira, pela dedicação ao meu projeto que me facilitou todo este processo (melhor equipa de aquisições de 2019). Finalmente, ao meu co-orientador Dr. Bruno Direito queria agradecer todo o apoio, persistência e supervisão. Tive muita sorte em ter decidido fazer o projeto de Mestrado neste centro de investigação e nas pessoas que me rodearam neste semestre.

Agradeço a todos os meus amigos que me acompanharam durante todos estes anos em Coimbra. Foi um processo longo que sem eles teria sido, com certeza, ainda mais longo. Desde as sessões de estudo pouco produtivas até a todas as noites académicas, vão ser as melhores memórias que levo da Universidade.

Gostava também de agradecer a todos os meus colegas de Engenharia Biomédica que fizeram parte do meu percurso.

Quero agradecer aos meus avós por terem mantido todo este tempo aquele olhar e discurso que diz "o meu netinho vai ser engenheiro!" que nunca desapareceu mesmo nos meus anos menos produtivos.

Finalmente, gostava de agradecer a paciência dos meus pais que, em retrospectiva, parece infundável. As oportunidades que me deram durante o curso foram essenciais para neste momento estar a concluir o meu ciclo de estudos com a confiança de saber o que eu quero que venha a seguir.





# Resumo

O neurofeedback (NF) é um procedimento experimental no qual a atividade neural medida é apresentada ao participante em tempo real na forma de uma representação auditiva ou visual, auxiliando na auto-regulação desses mesmos correlatos neurais de processos mentais. A variabilidade interindividual da eficácia e especificidade do neurofeedback ainda permanece uma questão importante que afeta a introdução do neurofeedback no contexto clínico. Estudos focados na investigação dos diferentes aspectos que influenciam o desempenho (como atenção, aspectos motivacionais e envolvimento da tarefa) estimam que o sucesso em neurofeedback varia entre 30 % e 50 %. O presente trabalho explora os correlatos neurais do feedback em relação às redes de recompensa e saliência e a sua associação com variações individuais associadas ao sucesso do treino cognitivo. Adquirimos dados anatômicos e funcionais de dez participantes saudáveis num paradigma de neurofeedback personalizado, com três tarefas distintas de imaginação de movimento. O paradigma do neurofeedback personalizado visa o aumento da motivação do participante e o empenho na tarefa e, conseqüentemente, o aumento do desempenho geral da neuromodulação. Os resultados mostraram ativações em áreas cerebrais relacionadas com a recompensa em relação com o feedback, que diferiram de acordo com o valor percebido da recompensa do feedback auditivo. Em última instância, este trabalho permitirá a otimização de parâmetros de neurofeedback personalizados e ajudará a definir potenciais biomarcadores de neuroimagem que sejam indicativos do sucesso do neurofeedback.

PALAVRAS-CHAVE: *fMRI, recompensa, aversão, auto-regulação, sucesso*



# Abstract

Neurofeedback (NF) is an experimental procedure in which measured neural activity is presented in the form of visual, auditory display to a participant in real-time, aiding on self-regulation of putative neural correlates of a given mental process. Individual variability of the efficacy and specificity of neurofeedback remains an important issue affecting the introduction of neurofeedback in the clinical context. Studies focused on the investigation of factors that affect performance (such as attentional variables, motivational aspects and task engagement) estimated success on neurofeedback experiments ranges between 30% and 50%. The present work explores the neural correlates of feedback concerning the reward and saliency networks and their association with individual variations associated with the success of the training. We acquired anatomical and functional data from ten healthy participants in a tailored neurofeedback paradigm with three distinct motion imagery tasks. The tailored neurofeedback paradigm aimed at the increase of participant's motivation and task engagement and, consequently, the increase in the overall performance in neuromodulation. The results showed activations in reward-related neural correlates concurrent with the feedback which differed according to the perceived reward-value of the auditory feedback. Ultimately, this research will allow the optimization of individually tailored neurofeedback parameters and help define potential neuroimaging biomarkers of neurofeedback success.

KEYWORDS: *fMRI, reward, aversion, self-regulation, success*



# List of Figures

2.1	Illustration of the haemodynamic response function (Barth and Poser 2011). . . . .	13
2.2	Illustration of types of experimental design used in fMRI-based Neurofeedback (Petersen and Dubis 2012). . . . .	14
2.3	Schematic illustration of the reward and aversion pathways in the reward circuit. <b>Legend:</b> <i>BLA: basolateral amygdala; CEA: central amygdala; CPu: caudate nucleus; DRN: Dorsal raphe nucleus; LDT: laterodorsal tegmental nucleus; LHA: lateral hypothalamus; LHb: lateral habenula; mPFC: medial prefrontal cortex; NAc: Nucleus Accumbens; OFC: orbitofrontal cortex; RMTg: rostromedial tegmental nucleus; SNc: substantia nigra pars compacta; VTA: ventral tegmental area</i> (as in Hu 2016). . . . .	17
2.4	Representation of key brain structures involved in different aspects of neurofeedback. <b>Reward processing:</b> Reported involvement of AAC and AIC in conscious perception of feedback and reward and VS involvement in reward processing; <b>Learning:</b> Dorsal striatum linked to neurofeedback learning; <b>Control:</b> dlPFC involvement in performance of executive tasks, attention to signal mediated by LOC and thalamus as a mediator of cortical arousal. <b>Legend:</b> <i>Anterior cingulate cortex (ACC), anterior insular cortex (AIC), Ventral Striatum (VS) / posterior parietal cortex (PPC), lateral occipital cortex (LOC), dorsolateral prefrontal cortex (dlPFC) / Dorsal striatum (DS)</i> . (as in T. e. a. Ros 2016). . . . .	18
3.1	The diagram represents the 5-point Likert Scale used to rate the reward-value of a subset of 20 vocalizations. Feedback sounds for the 3 different feedback types are defined according to each participant's rating. . . . .	20
3.2	The neurofeedback session timeline includes a priori feedback sound selection, an anatomical scan and 5 functional runs. . . . .	21
3.3	Equations for the calculation of the activation threshold of rewarding feedback for the condition 4OMI. . . . .	22

3.4	Feedback presentation scheme. Feedback threshold is defined in the and the events are defined as the moments when feedback is presented to the participant. The type of events will change based on the mean BOLD value (measured as a percentage of the BOLD signal variation) in the region of interest defined in bilateral area hMT+/V5. . . . .	24
4.1	Group ROI cluster. The legend refers to the degree of variability between selected target regions. . . . .	28
4.2	Group t-value statistics for the Training and Transfer runs. Values are presented as mean group value $\pm$ standard error of mean. . . . .	29
4.3	Group t-value statistics for the first and seconds NF runs. Values are presented as mean group value $\pm$ standard error of mean. . . . .	30
4.4	Group activation map for the Localizer run using as contrast (2OMS+4OMS>Stationary dot). The bilateral cluster shown in the activation map corresponds to the bilateral hMT+/V5 area (FDR $q < 0.05$ ) . . . . .	31
4.5	Activation maps for the Localizer run using the contrast (2OMS+4OMS>Stationary dot). The areas show in purple correspond to activated resulting from cluster thresholding ( $P < 0.004343$ , cluster threshold = 200 voxels). . . . .	31
4.6	Activation maps representing the cluster with positive t-values using the contrast (2OMI+4OMI>Stationary imagery) for the NF runs. The areas show in purple correspond to activated resulting from cluster thresholding ( $P < 0.001$ , cluster threshold = 200 voxels). . . . .	33
4.7	Activation maps representing the clusters with negative t-values peak activations in the NF runs using the contrast (2OMI+4OMI>Stationary imagery). The areas show in purple correspond to activated resulting from cluster thresholding ( $P < 0.001$ , cluster threshold = 200 voxels). . . . .	34
4.8	Activation maps representing clusters in the cerebrum for the event-related analysis referring to positive feedback concerning both NF runs. The areas show in green correspond to ROIs resulting from cluster thresholding ( $P < 0.001$ , cluster threshold = 300 voxels). . . . .	35
4.9	Activation maps representing clusters in the cerebellum for the event-related analysis referring to positive feedback concerning both NF runs. The areas show in green correspond to ROIs resulting from cluster thresholding ( $P < 0.001$ , cluster threshold = 300 voxels). . . . .	36
4.10	Activation maps for the event-related analysis referring to negative feedback events. Negative feedback events of both up-regulation tasks (2OMI+4OMI) in the two feedback runs were considered ( $P < 0.001$ , cluster minimum threshold = 300 voxels). . . . .	37

4.11 ERA of the three imagery tasks ROI with Tailarach coordinates (-60,-19,4) for both neurofeedback runs. The purple curve represents the ERA of the condition **4OMI**, the blue curve represents the ERA of condition **2OMI** and the brown curve represents the ERA of the condition **Stationary Imagery**. Black vertical lines represent the volume where the task block is initiated, following the presentation of the auditory cue (TR=0) and the end of the task block (TR=11). . . . . 40

4.12 ERA of the three imagery tasks ROI with Tailarach coordinates (9,5,1) for both neurofeedback runs. The purple curve represents the ERA of the condition **4OMI**, the blue curve represents the ERA of condition **2OMI** and the brown curve represents the ERA of the condition **Stationary Imagery**.Black vertical lines represent the volume where the task block is initiated, following the presentation of the auditory cue (TR=0) and the end of the task block (TR=11). . . . . 41

4.13 ERA of the three imagery tasks ROI with Tailarach coordinates (9,5,1) for both neurofeedback runs. The purple curve represents the ERA of the condition **4OMI**, the blue curve represents the ERA of condition **2OMI** and the brown curve represents the ERA of the condition **Stationary Imagery**.Black vertical lines represent the volume where the task block is initiated, following the presentation of the auditory cue (TR=0) and the end of the task block (TR=11). . . . . 42

4.14 ERA of the three imagery tasks in the the ventral anterior nucleus [TAL (9,-4,-7)] for both neurofeedback runs concerning the event-related negative feedback volume time course. The purple curve represents the ERA of the condition **4OMI**, the blue curve represents the ERA of condition **2OMI** and the brown curve represents the ERA of the condition **Stationary Imagery**.Black vertical lines represent the volume where the task block is initiated, following the presentation of the auditory cue (TR=0) and the end of the task block (TR=11). . . . . 43

4.15 ERA of both neurofeedback runs in the the anterior nucleus with [TAL (36,21,4)] The purple curve represents the ERA of the condition **4OMI**, the blue curve represents the ERA of condition **2OMI** and the brown curve represents the ERA of the condition **Stationary Imagery**.Black vertical lines represent the volume where the task block is initiated, following the presentation of the auditory cue (TR=0) and the end of the task block (TR=11). . . . . 44

A.1 Activation maps resulting from whole brain event-related analysis (SPM12) shows activated voxels in areas such as the orbitofrontal cortex ( $T=3.94$ ,  $p<0.001$ ) and the cingulum ( $T=3.35$ ,  $p<0.001$ ). Anatomical identification was performed based on MNI coordinates and the AAL toolbox. . . . . 56



# List of Tables

4.1	T-test comparison for the group t-values of all participants between the Training and Transfer runs. . . . .	28
4.2	Peak voxels of activated cerebral regions, associated BAs and tailarach coordinates for the block analysis referring to the Localizer run ( $P < 0.004343$ , cluster minimum threshold = 200 voxels). . . . .	32
4.3	Peak voxels of activated cerebral regions, associated BAs and tailarach coordinates for the block analysis referring to both NF runs ( $P < 0.001$ , cluster minimum threshold = 200 voxels). . . . .	33
4.4	Peak voxels of negative t-values for the contrast of interest. The cerebral regions, associated BAs and tailarach coordinates for the block analysis referring to both NF runs are identified. ( $P < 0.001$ , cluster minimum threshold = 200 voxels). . . . .	34
4.5	Peak voxels of activated cerebral regions, associated BAs and tailarach coordinates for the event-related analysis referring of positive feedback . Positive feedback events of both up-regulation tasks (2OMI+4OMI) in the two feedback runs were considered ( $P < 0.001$ , cluster minimum threshold = 300 voxels) . . . . .	35
4.6	Peak voxels of activated cerebellar regions, associated BAs and tailarach coordinates for the event-related analysis referring of positive feedback. Positive feedback events of both up-regulation tasks (2OMI+4OMI) in the two feedback runs were considered ( $P < 0.001$ , cluster minimum threshold = 300 voxels) . . . . .	36
4.7	Peak voxels of activated cerebral regions, associated BAs and tailarach coordinates for the event-related analysis referring to negative feedback. Negative feedback events of both up-regulation tasks (2OMI+4OMI) in the two feedback runs were considered ( $P < 0.001$ , cluster minimum threshold = 300 voxels). . . . .	37
B.1	Participants details. Participants are described according to gender, age, dominant hand (laterality) and their previous experience with rtfMRI or NF sessions.	58

C.1	Individual ROI-GLM statistics for each participant for the training run. The t-values and p-values presented refer the NF target and the contrast (4OMI+2OMI > Stationary Imagery) . . . . .	59
C.2	Individual ROI-GLM statistics for each participant for the transfer run. The t-values and p-values presented refer the NF target and the contrast (4OMI+2OMI > Stationary Imagery) . . . . .	60
C.3	Individual ROI-GLM statistics for each participant for the first neurofeedback run. The t-values and p-values presented refer the NF target and the contrast (4OMI+2OMI > Stationary Imagery) . . . . .	61
C.4	Individual ROI-GLM statistics for each participant for the second neurofeedback run. The t-values and p-values presented refer the NF target and the contrast (4OMI+2OMI > Stationary Imagery) . . . . .	62

# Contents

<b>List of Figures</b>	<b>xi</b>
<b>List of Tables</b>	<b>xv</b>
<b>1 Introduction</b>	<b>1</b>
1.1 Motivation and Relevance . . . . .	2
1.2 Main contributions . . . . .	2
1.3 Research Questions . . . . .	3
<b>2 Neurofeedback and the reward system: understanding neural correlates and improving efficacy</b>	<b>5</b>
2.1 Neurofeedback . . . . .	5
2.1.1 Brain activity as the source of biofeedback . . . . .	5
2.1.2 Neurofeedback systems and the evolution of imaging modalities	6
2.1.2.1 EEG-based Neurofeedback . . . . .	7
2.1.2.2 rtfMRI-based Neurofeedback . . . . .	8
2.1.3 Neurofeedback protocol . . . . .	8
2.1.4 Factors in Neurofeedback Design . . . . .	9
2.1.5 Factors in Neurofeedback Success . . . . .	10
2.2 fMRI-based Neurofeedback . . . . .	12
2.2.1 Magnetic Resonance Imaging Principles . . . . .	12
2.2.2 Functional Magnetic Resonance Imaging . . . . .	12
2.2.3 Experimental protocol design in NF . . . . .	14
2.3 Reward System . . . . .	15
2.3.1 Reward system and reinforcement learning . . . . .	15
2.3.2 Neural Correlates . . . . .	15
2.3.3 Reward and learning: role in neurofeedback . . . . .	16
<b>3 Methods</b>	<b>19</b>

3.1	Participants . . . . .	19
3.2	Experimental Protocol . . . . .	20
3.2.1	Structural run . . . . .	21
3.2.2	Functional runs . . . . .	21
3.2.2.1	Functional localizer . . . . .	22
3.2.2.2	Imagery runs . . . . .	23
3.2.3	Online fMRI processing . . . . .	24
3.2.3.1	ROI functional definition . . . . .	25
3.2.4	Data analysis . . . . .	25
<b>4</b>	<b>Results</b>	<b>27</b>
4.1	Group ROI analysis . . . . .	27
4.1.1	ROI localization . . . . .	27
4.1.2	Learning effects . . . . .	28
4.1.3	Self-regulation performance . . . . .	29
4.2	Whole-brain group analysis . . . . .	30
4.2.1	Block protocol activation maps . . . . .	30
4.2.1.1	Localizer run . . . . .	30
4.2.1.2	Feedback runs . . . . .	33
4.2.2	Event-related protocol activation maps . . . . .	35
4.2.2.1	Positive feedback events . . . . .	35
4.2.2.2	Negative feedback events . . . . .	37
4.2.3	Event-related averaging time course analysis . . . . .	39
4.2.3.1	Primary Auditory Cortex (Brodmann Area 22) . . . . .	40
4.2.3.2	Caudate . . . . .	41
4.2.3.3	Thalamus . . . . .	43
4.2.3.4	Insula . . . . .	44
<b>5</b>	<b>Discussion</b>	<b>45</b>
<b>6</b>	<b>Conclusions</b>	<b>49</b>
	<b>Appendices</b>	<b>53</b>
A	Pilot Studies . . . . .	55
B	Participants details . . . . .	58
C	Individual ROI-GLM Statistics . . . . .	59

# Introduction

Imaging techniques have emerged as an essential part of the study of brain structure and function since the second half of the 20<sup>th</sup> century. Imaging modalities have been used in complementary ways to give insight into the different structural and functional organization aspects of the nervous system (Latchaw, Kucharczyk, and Moseley 2005).

## **Neuronal plasticity**

The discovery of processes underlying neuronal plasticity as a substrate for structural and functional reorganization through learning processes or adaptation to injury has earned the attention of scientists as a potential gateway for promising interventions for neurorehabilitation. Harnessing the potential of brain plasticity, new neuroscience-driven clinical applications have emerged (Nava and Röder 2011).

## **Imaging and Neurofeedback**

The identification of a relationship between neural activation and performance of tasks led to the development of neurofeedback. This procedure aims at modulating the intensity of task-specific brain activation to improve normal function or correct functional abnormalities or enhance performance in health and disease (Sulzer et al. 2013). Neurofeedback experiments were first performed with Electroencephalography (EEG) (Elbert et al. 1980). The evolution of imaging techniques and computation speed resulted in the advent of new neuroimaging modalities such as real-time functional Magnetic Resonance Imaging (rtfMRI), which presents an enhanced spatial resolution and wider brain coverage compared to EEG. RtfMRI neurofeedback enabled the target of specific subcortical brain regions and increased the potential of neurofeedback as an instrument for neuroimaging research.

Despite the promise of being a tool for neurorehabilitation, rtfMRI-based neurofeedback is limited in its efficacy with estimated moderate percentages of participant's success (Niv 2013). The understanding of the causes of inter-subject variability is key to increase its success and propel neurofeedback to the status of an established clinical therapy.

## 1.1 Motivation and Relevance

The introduction of a non-invasive mechanism-driven alternative in the clinical context to correct neurophysiological abnormalities has been the main goal of researchers since the advent of neurofeedback. Despite its non-invasive nature, absence of negative pharmacological effects and results in brain modulation activity with behavioural changes associated with it, the reduced efficacy of this experimental procedure remains a caveat in the field (Niv 2013). The estimated efficacy of 50%-70% prevents the introduction of NF training in the clinical setting (Kadosh and Staunton 2018). The identification of brain structures involved in feedback processing and their association with the individual success in NF training may serve as the basis for the development of a new tailored NF experimental designs which aim at decreasing inter-individual variability effects in overall self-regulation performance. The present contribution identifies the neural correlates of feedback in relation to the reward and salience networks in rtfMRI-based neurofeedback (Menon 2015) and the putative association with individual variations associated with the success of the neurofeedback training. Following the main purpose, the structures identified in this study may be utilized to tailor neurofeedback experiments to achieve higher rates of neurofeedback success.

## 1.2 Main contributions

The main contributions of the present work are:

- Identification of neural correlates associated with feedback events with different reward-values during neurofeedback sessions;
- Proof-of-concept study for the establishment of neuroimaging biomarkers to allow the implementation of individually tailored neurofeedback session to the participant.

## 1.3 Research Questions

The research questions the present work intends to answer are:

1. Is it possible to identify neural correlates of learning processes related to the moments when participants receive feedback information during a neurofeedback experiment?
2. How do the neural correlates of feedback events relate to neurofeedback success within a session?





# Neurofeedback and the reward system: understanding neural correlates and improving efficacy

## 2.1 Neurofeedback

### 2.1.1 Brain activity as the source of biofeedback

Biofeedback is a non-invasive technique that allows a subject to receive information about a specific physiological variable that is being measured during a certain amount of time allowing the subject to attempt to modify it accordingly to a pre-defined activation goal (Sitaram, T. Ros, et al. 2016). Neurofeedback is a form of biofeedback which uses as variable the brain activity of a specific brain area. This procedure allows for self-regulation of brain activity with possible lasting effects on behavior (Weiskopf 2012).

A variety of theories exist suggesting explanations for the process of learning during neurofeedback sessions(Sitaram, T. Ros, et al. 2016:

- Operant or instrumental learning: states that the reward of achievement of target brain activation levels by means of feedback leads to learning of neuromodulation (Skinner 1945). In this way, the participant learns how to correctly neuromodulate by making an association between the brain response and the respective feedback which acts as a reinforcer(T. e. a. Ros 2016).
- Motor learning: states the learning of regulation of neurophysiological signals resembles the acquisition of motor learning of movement sequences.
- Dual process theory: the complementation of feedback and feedforward processes leads the participant to learning. The participant's search for an effective mental strategy to control the feedback signal is mediated by processes of feedforward when a successful strategy is discovered and its reinforcement by feedback leads to an automatization of such strategy.
- Awareness theory: states the control of brain activity results from the awareness of the brain activity itself and not an mental strategy. This theory is

adversarial to the operant learning model.

- Global workspace theory: states that a global distribution of structures in the brain play a role in feedback processing in the brain which leads to a conscious learning of brain self-regulation. This theory complements the operant learning model, by adding external brain structures feedback processing and consciousness to the process of learning.
- Skill learning: states that neurofeedback learning is a skill, which involves a initial rapid improvement and slowly starts to become consolidated over time.

The most prominent theory is the "operant learning theory", which states that the reward of achievement of target brain activation levels by means of feedback leads to learning of neuromodulation (Skinner 1945). In this way, the participant learns how to correctly neuromodulate by making an association between the brain response and the respective feedback which acts as a reinforcer (T. e. a. Ros 2016).

Nevertheless, theories such as the global workspace theory and the dual process theory become complementary of the operant learning theory.

This study is focused on the principles of the operant learning and global workspace theory, studying the role of the reward system in feedback processing and performance success.

## **2.1.2 Neurofeedback systems and the evolution of imaging modalities**

Brain activity is measured based on changes in the membrane potential of activated neurons (using electrophysiological methods) or based on changes in energy metabolism required to activate neurons (hemodynamic methods). A wide variety of non-invasive techniques allow the indirect measurement of electrical, magnetic and metabolic variations. Two of these techniques are referred below are briefly explained in association with NF: EEG and fMRI.

### **2.1.2.1 EEG-based Neurofeedback**

EEG is a non-invasive electrophysiological technique which measures brain electrical activity on the surface from the scalp. This method is based on the fact that a population of underlying neurons activated synchronously leads to a considerable summed electrical activity which leads to an electrical signal in the superficial extracellular space near the skin. Therefore, the recorded brain waves are indicative of fluctuations of excitability in neuronal populations and its signal represents the sum of excitatory or inhibitory postsynaptic potentials (Beres 2017). The recording

of the electric field is performed using electrodes on the scalp of the participant and electrical changes are measured comparing with a reference electrode.

Historically, electroencephalography-based neurofeedback (EEG-NF) was the first method used to implement neurofeedback (Elbert et al. 1980). Positive results have been reported in the application of EEG-NF in treatment of neurological disorders such as epilepsy (Walker and Kozlowski 2005), attention deficit hyperactivity disorder (Shereena et al. 2019), autism spectrum disorder (Kouijzer et al. 2013), depression (Linden 2014), anxiety (Moradi et al. 2011), chronic pain (Hassan et al. 2015), traumatic brain injury (Gray 2017), dyslexia (Breteler et al. 2010), brain stroke (Mottaz et al. 2018) and Alzheimer's disease (Jiang, Abiri, and Xiaopeng Zhao 2017).

Three types of EEG-NF protocol are in use nowadays, which modulate different electrophysiological parameters (Omejc et al. 2018):

- Slow cortical potentials (SCPs) training: Protocol aims at the indirect regulation of cortical excitability by self-modulation of specific event-related potentials denominated SCPs. This training is based on association between variation of SCPs and the effects on information processing (Gevensleben et al. 2014). SCPs may be negative or positive, indicating lowered or increased thresholds for excitation of neuronal structures respectively. The thresholds for excitation influence, in turn, information processing either by facilitating it (low threshold) or hindering it (high threshold).
- Coherence training: Protocol aims at regulating connectivity activation patterns among different brain structures. For this purpose, the correlation of brainwaves of specific brain structures is measured concerning aspects such as phase, amplitude and frequency. The rationale for this type of training results from the observation of distorted connectivity activation patterns in neurological disorders when comparing with healthy controls.
- Frequency training: Protocol targets the power ratio between specific EEG frequency bands. The hypothesis behind this training protocol is the association of amplitudes of different types of frequencies with a corresponding cognitive function. Brain waves with different frequency bands have been observed during EEG: delta (less than 3Hz), theta (4-8 Hz), alpha (8-12 Hz), beta (12-30 Hz) and gamma (higher than 30 Hz).

EEG-NF still is the most widely used neurofeedback type. However, its inherent characteristics of measuring neuroelectrical signals with a limited number of electrodes placed on the surface of the scalp lead to reduced performance in localizing active brain areas, especially for deep subcortical areas.

### 2.1.2.2 rtfMRI-based Neurofeedback

The development of new imaging modalities such as functional magnetic resonance imaging (fMRI) and the advancement of computation hardware and processing speed, resulted in the advent of real time fMRI (rtfMRI) (Cox, Jesmanowicz, and Hyde 1995), enabling tracking brain activity of both cortical and subcortical circumscribed areas and online processing of functional images in a MRI scanner (Weiskopf 2012). The application of the principles of neurofeedback with rtfMRI resulted in studies reporting successful modulation in areas such as the primary motor and pre-motor areas (Scharnowski, Veit, et al. 2015), anterior insula (Caria et al. 2010), visual cortex (Scharnowski, Hutton, et al. 2012) and prefrontal cortex (Zhang et al. 2013).

More recently, self-regulation of brain networks using information concerning the interaction between brain areas has become a trend in rtfMRI NF studies (Xiaojie Zhao et al. 2013, Koush et al. 2013).

### 2.1.3 Neurofeedback protocol

Neurofeedback experimental protocols vary according to the task. Nevertheless, neurofeedback sessions adopt a similar framework as reference (Sulzer et al. 2013):

- Definition of a region-of-interest, either functionally or by means of an anatomical reference, which will be the target of modulation training;
- A training run is executed before feedback runs in which the participant is unaware of its performance. This run will serve as a reference to prove feedback runs success and behavioral change post-training;
- Presentation of real-time online information of the ROI's activity to the participant. The ROI's activity is presented to the participant in the form of a representation which translates the percentage of activation relative to the pre-defined target activation level of the task. This representation takes the form of a stimulus which can be visual, auditory, haptic or electrical and its purpose is to ease participant's comprehension of the information received. After receiving the information, the participant will attempt to modulate activation in the ROI using mental strategies based on the feedback;
- After feedback training, a transfer run is performed to ensure the participant did learn a skill to control brain activity and can perform such skill absent of feedback;
- Implementation of control conditions to account for confounds and minimize bias in results (Sorger, Scharnowski, et al. 2019);

- Test for behavioral effects after session in relation to the baseline performance.

### 2.1.4 Factors in Neurofeedback Design

Neurofeedback consists of an experimental procedure which lasts from minutes to hours and should follow a specific study design. A variety of factors should be taken into consideration to maximize its efficacy (Sorger, Scharnowski, et al. 2019). Such factors include:

- Feedback approach - Feedback is given to the participant in a way the participant can perceive the levels of activation of the target area whilst executing a mental strategy that he/she learns to change such activation levels. An explanation about the ROI functional role and a suggestion of potential mental strategies to modulate it can be presented to the participants before the session (explicit) or otherwise success in ROI modulation can result from in-session "trial and error" operant learning (implicit).
- Perception of success and motivation - Participant's engagement in task and motivation may affect performance.
- Non-Specific Effects - Effects due to factors non-related with the task execution should be minimized to ensure a replicable relationship between the participant's target brain region activity levels and the results obtained during feedback training. The minimization of the effects may require monitoring of the factors during the session coupled with post-session processing.
- Specificity of ROI - The extent to which the feedback from a particular ROI and its specificity in processing a particular cognitive aspect is important to reach the desired target activation levels or the specified behavioral change.
- Expectation Effects - Placebo effects due to the technological setup where neural modulation occurs may affect the behavioral change that transfers to real-life settings after feedback training.
- Behavioral effects unrelated to feedback per se - The extent to which feedback training results differ from results using other mental strategies and training (Dewiputri and Auer 2013).
- Adaptive difficulty level - Definition of thresholds adapted to e.g. each participant, specific ROIs.

All these factors are related to study design and should be considered. In particular, the perception of success by the participant is a factor which depends not only on the experimental design but also the capability of the participant to correspond to the goals of the experiment. Consequently, it is closely linked with a relevant intersubject variability.

### 2.1.5 Factors in Neurofeedback Success

Currently, neurofeedback does not have results in a significant part of the population that undergoes study, varying from 50 to 70 % (Kadosh and Staunton 2018). Seeing that such a significant part of the population does not respond to neurofeedback treatment ("non-performers"), a need to understand what drives such variability in-between subjects in neurofeedback performance is made relevant. In the review *Kadosh and Staunton 2018*, the author addresses the inefficacy problem of neurofeedback as a experimental procedure using results of EEG-based and rtfMRI-based neurofeedback studies. In this sense, the author points out the latest evidence on the effects of psychological factors in NF performance (independent of the basis imaging modality or technique) and refers to them as a priority to address inter-subject variability, emphasizing the possibility of modulation of these factors for the optimization of results.

The psychological factors identified in the review include attention, motivation, mood and personality factors. In terms of correlation with performance and learning in neurofeedback training, attention has been the most influential psychological variable. It also has a high correlation with the level of motivation and engagement on the task by the participant. Aspects such as confidence in mastery of a task, interest in the task at hand, fear of failing and the perceived degree of challenge of a task have been implicated in altering the performance of participants. Fear of incompetence harms performance and is amplified during the course of the feedback run by poor results with negative influence over confidence of mastering the task. The fact that psychological variables influence outcomes suggests that the best approach to neurofeedback training should include personalized study design according to each participant's characteristics. The maximization of the efficiency of training not only includes considerations in overall design by minimizing distractions and optimizing feedback for the task's purpose but also an adaptation to participant's capability of neural activity modulation and psychological factors to maximize engagement with the task, minimize frustration and increase the success rate of training (Alkoby et al. 2018).

## 2.2 fMRI-based Neurofeedback

### 2.2.1 Magnetic Resonance Imaging Principles

Matter is constituted by atoms, which in turn have electrically charged components (electrons and protons). These components have intrinsic angular moments (spins) different from 0 but normally the spin of the components in an atom tend to cancel each other due to the fact they are directed at random directions. However, when in the presence of an external magnetic field, the nuclear spin of these components tend to line up with the direction of the field and spin with a frequency which depends on the field strength. This alignment leads to a change in net magnetization thus creating a magnetic signal. Adding a transversal radiofrequency (RF) pulse causes the components to be unaligned with such field. When the RF pulse is turned off, the components recover until they realign with the external magnetic field and, in the process, create a decaying signal.

In Magnetic Resonance Imaging (MRI), the relaxation time constants  $T_1$ ,  $T_2$  and  $T_2^*$  are measured:

- $T_1$  refers to the recovery of vertical magnetization following the end of the RF pulse.
- $T_2$  refers to the quick dephasing which occurs due to the loss of coherence between different spins after the RF pulse is turned down.
- $T_2^*$  refers to the transverse magnetization observed due to interactions on the atomic level.

The amplitude of the measured signal as well as the relaxation time constants change according to the properties of the tissues where the nuclei are embedded. This allows for the establishment of contrasts and extraction of high resolution anatomical spatial information in the form of three-dimensional images (Brown, Cheng, and Haacke 2018).

### 2.2.2 Functional Magnetic Resonance Imaging

The functional MRI (fMRI) extends the principles of MRI referred above coupled to the fact that blood presents a different magnetic susceptibility compared to the surrounding tissues in the brain which changes according to neuronal activity. Active neurons have higher metabolic demands than inactive neurons which require more energy. Since neurons are not able to store energy, there is a need for an increase in blood flow concurrent with the activation of these neurons. The blood flow increase brings more oxygen in the form of oxygenated hemoglobin. The variation in the

net value of oxygenated hemoglobin causes inhomogeneity in the nearby magnetic field, leading to measurable changes in the magnetic signal. This variation is called hemodynamic blood oxygen level-dependent (BOLD) signal (Barth and Poser 2011). These variations influence  $T2^*$ , allowing for the generation of contrasts (Logothetis and Wandell 2004).

The reduction of the minimum repetition time, the increase in computational power and its effect on the reduction of the length of analysis and processing of data as well as developments in the scanners have potentiated the advent of rtfMRI. The reduction of repetition time (TR) to a minimum of 2 seconds and the online analysis and processing of the data allow the introduction of experimental protocols where the participant receives online information during the session (Sitaram, Lee, et al. 2011).

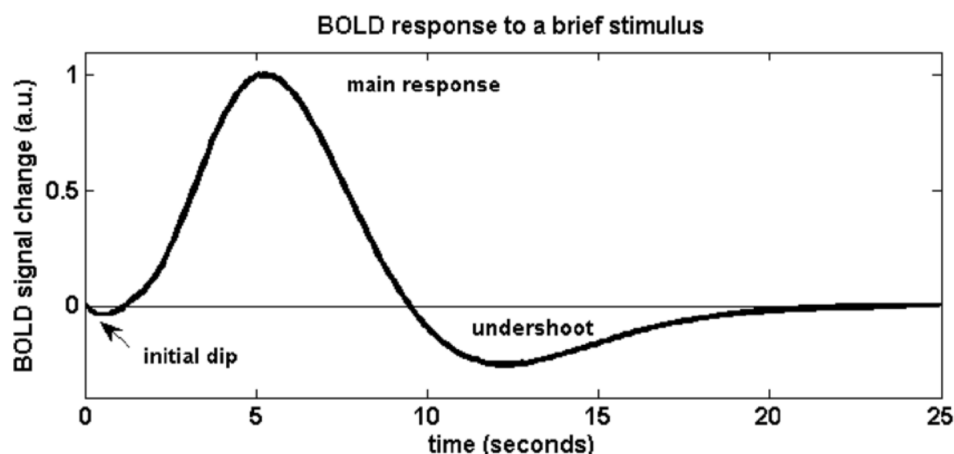


**Figure 2.1:** Illustration of the haemodynamic response function (Barth and Poser 2011).

The timecourse of the BOLD signal is known as a hemodynamic response function (HRF) and resembles the response function presented in Figure 2.1. The function initiates with a short-lived decrease in signal (so-called “dip”) before cerebral blood flow increase followed by an overshoot with a peak after 3 to 6 seconds and finally followed by a post-stimulus undershoot (Barth and Poser 2011).

### 2.2.3 Experimental protocol design in NF

The experimental protocol varies according to the goal of the experimental setup (Petersen and Dubis 2012). Most widely used protocols in rtfMRI NF include block protocol and event-related protocol (Dale and Buckner 1997; Maus et al. 2010).

The block design is organized in several trials of the same type and reduced duration (15-50 seconds) conducted sequentially and the responses during the session are



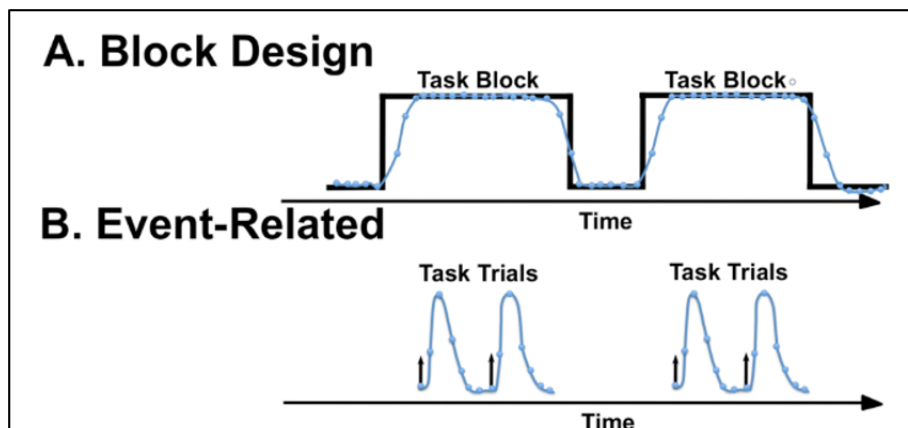


**Figure 2.2:** Illustration of types of experimental design used in fMRI-based Neurofeedback (Petersen and Dubis 2012).

averaged over all trials (Figure 2.2 A). This approach allows to establish task-specific conditions and leads to better signal-to-noise ratios. This design is often applied to localize functional areas or model sustained activity brain processes. Block design analyzes differential activity between task blocks, with standard protocols including control task blocks interleaved with activation blocks or regulation control (Sorger, Scharnowski, et al. 2019).

With the improvement of fMRI sampling and analysis strategies, the event-related design became increasingly more popular. This design measures transient activity due to an short-lived stimulus that may last only a couple of seconds (Figure 2.2 B). The resolution improvement results smaller intervals between similar tasks with minimums depending only upon the BOLD response function duration. This design type allows a random presentation of stimuli with no need of *a priori* definition. Limitations to this design include a reduced signal-to-noise ratio due to a reduced number of events.

The mixed design results from a combination of the block design and event-related design, where different types of events occur within predefined task blocks, accounting for both transient and sustained activity (Petersen and Dubis 2012).

## 2.3 Reward System

### 2.3.1 Reward system and reinforcement learning

The reward system consists of a network of brain structures that activate when action outcomes surpass predicted value, which is important to guide motivated goal-directed actions (Sescousse, Li, and Dreher 2013). Reward is therefore intimately related to the concept of motivation which is essential for adaptive behavior (Sutton and Barto 1998).

The principle of learning associated with the effect of neurofeedback training is referred to as operant learning (also known as reinforcement learning) and is based on the association between two stimuli in which a reinforcing stimulus leads to an expected physiological change in neural activity (Sulzer et al. 2013).

### 2.3.2 Neural Correlates

The concept of an anatomically identifiable reward circuit was first introduced by *Olds and Milner 1954* and was later corroborated by pharmacological studies (Phillips and Fibiger 1978 , Bevan, Smith, and Bolam 1996). The reward system is constituted mainly by the cortical-basal ganglia circuit which includes the anterior cingulate cortex (ACC), the orbital prefrontal cortex (OFC), the ventral striatum (VS), the ventral pallidum (VP) and the midbrain dopamine neurons (Haber and Knutson 2010). This network of brain structures plays key roles in reward anticipation and reinforcement learning and is separated into two major pathways (Alexander and Crutcher 1990):

- **Mesolimbic dopamine pathway:** Projections initiate in ventral tegmental area (VTA) and terminate in nucleus accumbens (NA);
- **Mesocortical dopamine pathway:** Projections initiate in the VTA and terminate in different areas of the prefrontal cortex (PFC). These areas include the anterior cingulate cortex (ACC), the anterior insular cortex (AIC) and orbitofrontal cortex (OFC).

Both pathways function in parallel encoding reward (mesolimbic) and effort prediction (mesocortical), with information on both aspects integrated in the VS for decision-making (Hauser, Eldar, and Dolan 2017). For the purpose of directing goal-oriented behaviour and reinforcing learning, the organization of this circuit is interwoven with sensorimotor and associative circuits (Gremel and Lovinger 2017). The functional connection of these circuits is essential for stimulus-response associations (sensorimotor circuit) and response-outcome associations (associate circuit)

which regulate decision-making (Redgrave et al. 2010).

Complementing the main dopamine pathways, other brain areas have reported regulatory roles in the reward circuit (Figure 2.3) :

- **Amygdala:** Subregions of the amygdala present different roles in the reward system. The basolateral amygdala is linked to the association of sensory information with reward and the modification of the reward value of an outcome based on motivational aspects. The central amygdala is linked to reinforcement of reward dependent on the motivational state (Chesworth and Corbit 2017).
- **Hippocampus:** Hippocampal synapses connecting to the nucleus accumbens (NAc) in the VS (LeGates et al. 2018) and the existence of reward-predictive cells in the CA1 subfield and subiculum (Gauthier and Tank 2018) indicate a role in reward processes.
- **Lateral habenular nucleus (LHb):** Activations contingent on negative valence reward-related signals (Ullsperger and Von Cramon 2003) indicate an indirect modulatory role in the reward-related dopamine signal (Araki, McGeer, and Kimura 1988).
- **Pedunculopontine tegmental nucleus (PPT):** Relay structure for strongest excitatory input to dopamine neurons in substantia nigra (SNc) and potential involvement in the computation of the difference between the reward expected and the actual reward received (Kobayashi and Okada 2007).
- **Raphe nucleus (RN):** The dorsal subregion of the raphe nucleus mainly comprises serotonergic innervations. Several studies report involvement with a variety of reward-related processes, including modulation of reward value and encoding of expected and actual rewards (Nakamura, Matsumoto, and Hikosaka 2008).

### 2.3.3 Reward and learning: role in neurofeedback

Several brain areas in the reward system have been linked to aspects of neurofeedback, including reinforcement learning, reward processing and neurofeedback control (represented in Figure 2.4).

In the article Sorger, Kamp, et al. 2018, the effectiveness of neurofeedback in enhancing self-regulation of brain activity has been established when compared with other cognitive strategies, independent of ROI and functional task. Furthermore, the use of a parametric activation paradigm appears to further facilitate the success of the neurofeedback session when compared with standard up-regulation/down-regulation paradigms. The parametric activation paradigm suggests that a higher perceived

## 2. Neurofeedback and the reward system: understanding neural correlates and improving efficacy

---

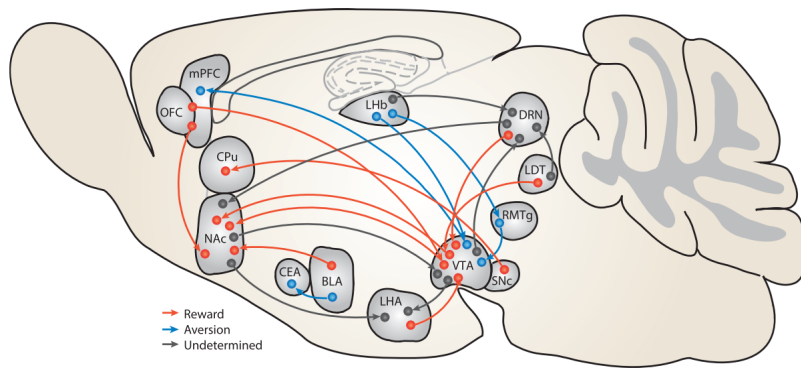


**Figure 2.3:** Schematic illustration of the reward and aversion pathways in the reward circuit. **Legend:** *BLA*: basolateral amygdala; *CEA*: central amygdala; *CPu*: caudata nucleus; *DRN*: Dorsal raphe nucleus; *LDT*: laterodorsal tegmental nucleus; *LHA*: lateral hypothalamus; *LHb*: lateral habenula; *mPFC*: medial prefrontal cortex; *NAc*: Nucleus Accumbens; *OFC*: orbitofrontal cortex; *RMTg*: rostromedial tegmental nucleus; *SNC*: substantia nigra pars compacta; *VTA*: ventral tegmental area (as in Hu 2016).

challenge of the task positively influences the performance in neurofeedback, which is in accordance with reported results of previous studies (referred in the section 2.1.5).

In a recent study *Skottnik et al. 2019* addressed the success in neurofeedback sessions with visual feedback when compared with other techniques of neuromodulation absent of feedback and revealed an overall increase in activation in areas such prefrontal control regions, anterior insula and visual cortices as well as decreased activations in the default mode network and the posterior insula, all of which involved in visual information processing (Gattass et al. 2005) or reward-related processes (Haber and Knutson 2010). The anterior striatum showed significant increases in activations correlated with success in neurofeedback sessions when compared with other cognitive strategies.

## 2. Neurofeedback and the reward system: understanding neural correlates and improving efficacy

---

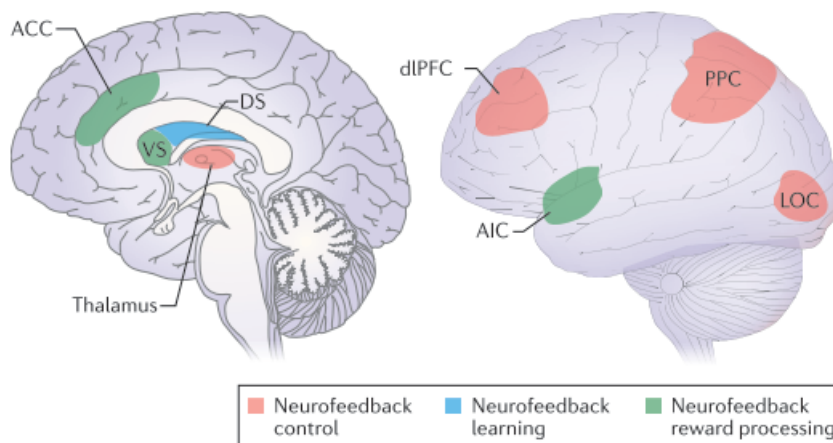


**Figure 2.4:** Representation of key brain structures involved in different aspects of neurofeedback. **Reward processing:** Reported involvement of AAC and AIC in conscious perception of feedback and reward and VS involvement in reward processing; **Learning:** Dorsal striatum linked to neurofeedback learning; **Control:** dlPFC involvement in performance of executive tasks, attention to signal mediated by LOC and thalamus as a mediator of cortical arousal. **Legend:** Anterior cingulate cortex (ACC), anterior insular cortex (AIC), Ventral Striatum (VS) / posterior parietal cortex (PPC), lateral occipital cortex (LOC), dorsolateral prefrontal cortex (dlPFC) / Dorsal striatum (DS). (as in T. e. a. Ros 2016).

## 2. Neurofeedback and the reward system: understanding neural correlates and improving efficacy

---

# 3

## Methods

### 3.1 Participants

10 participants with no history of neurological or psychiatric disorders were included in this study (5 male and 5 female). Participants' ages ranged between 19 and 35 years old (mean age = 26, SD = 5.25) and the majority was right-handed (1 participant was left-handed). Only 2 of the participants had previously been part of any rt-fMRI neurofeedback. The participants details are presented in table B.1 in the *Appendices*.

Before the start of the scanning session, the participants were informed of the visual and imagery tasks to perform and different types of auditory cues. Additionally, participants were asked to identify from a subset of 20 vocalizations the most rewarding, penalizing and neutral vocalization. The subset was obtained from the database available in Cowen et al. 2018. The process of identification was a Likert-type scale questionnaire in which participants rated each vocalization from 1 (most punishing) to 5 (most rewarding). A follow-up questionnaire presented the participants with all vocalizations previously rated with the same numerical classification (only for classifications 1,3 and 5) to allow the selection of one vocalization for each classification to be used as auditory feedback in the neurofeedback runs (Figure 3.1).

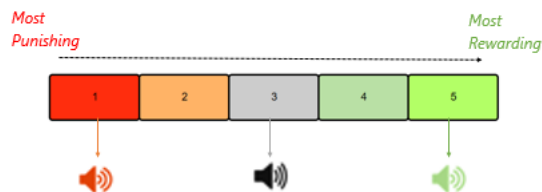


**Figure 3.1:** The diagram represents the 5-point Likert Scale used to rate the reward-value of a subset of 20 vocalizations. Feedback sounds for the 3 different feedback types are defined according to each participant's rating.

Pilot studies were performed to test and optimize the experimental protocol in 2 participants which are not included in the results. Information about the pilot

studies is presented in section A in the *Appendices*.

## 3.2 Experimental Protocol

Each session consisted of an anatomical scan and 5 functional runs: a bilateral hMT+/V5 functional localizer and 4 imagery runs (Figure 3.2). The first and last imagery runs were presented without feedback information. The remaining two functional runs are neurofeedback runs.

Both anatomical and functional runs were performed in a 3 Tesla Siemens Magnetom Scanner using a 20-channel head coil.

The following experimental protocol is based on a previously used protocol of Sousa et al. 2016 complemented with new features in the Neurofeedback (NF) runs and offline analysis in order to adapt it to the research question of the present work. All modifications in the protocol design were coded using MATLAB 2014a (MathWorks) and the PsychoPhysics Version 3 toolbox (<http://psychtoolbox.org/>). The modifications in the experimental protocol are presented briefly below:

- A priori selection of personalized sound for feedback presentation by feedback type (positive, neutral and negative). The sounds introduced in this study were cross-culturally validated human vocalizations of emotion made available in the article Cowen et al. 2018;
- Presentation of feedback in a predefined volume (5 TR and 9 TR) for each task block. In the previous experimental protocol, feedback was given by the directly by the experimenter by voice and expressed the quantitative change in the signal (experimenter express changes in self-regulation as increases or decreases based on the defined baseline level).
- Introduction of a personalized threshold of activation for each participant according to its own self-regulation capabilities. This new feature intended to address inter-subject variability by challenging each participant according to their own self-regulation ability established on a imagery task in the first functional run.

Experimental sessions were conducted using Turbo-BrainVoyager Version 3.2 (Brain Innovation, Maastricht, The Netherlands) which was used for real-time fMRI data processing, MATLAB 2014a (MathWorks) for stimulus and feedback display and NeuroElf Version 1.1 Toolbox (<http://www.neuroelf.net/>) for threshold feedback calculation.



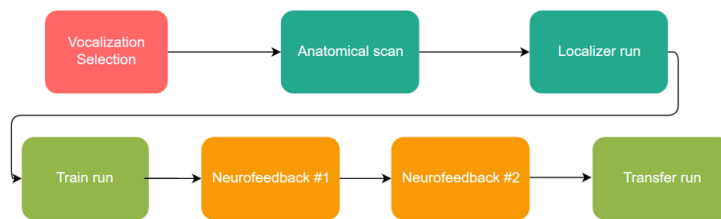


**Figure 3.2:** The neurofeedback session timeline includes a priori feedback sound selection, an anatomical scan and 5 functional runs.

### 3.2.1 Structural run

Each session started with the acquisition of a high-resolution magnetization-prepared rapid acquisition gradient echo (MPRAGE) sequence for co-registration of functional data (176 slices; Repetition Time (TR): 2530 ms; Echo Time (TE): 3.42 ms; Voxel size: 1.0 x 1.0 x 1.0 mm<sup>3</sup>; Flip Angle (FA): 7°; Field of view (FOV): 256 x 256 mm<sup>2</sup>).

### 3.2.2 Functional runs

Functional images obtained consisted of 33 slices (FOV: 256x256 mm<sup>2</sup>, voxel size 4.0 x 4.0 x 3.0 mm<sup>3</sup>, FA: 90°, TR: 2000 ms; TE: 30 ms) covering the occipital and posterior temporal lobe.

The order of up-regulation tasks in each functional run was randomized for each participant and interspersed by a block of down-regulation tasks in order to avoid prediction of the upcoming task by the participant and to further ensure that the performance relates to the task.

#### 3.2.2.1 Functional localizer

The functional localizer was composed of 200 volumes and used a moving dot task to activate the bilateral hMT+/V5 area which is the target region for neurofeedback. The selection of the neurofeedback target area was based on the fact this is a well-studied area sensitive to motion which has been previously easily identifiable through functional visual localizers with motion selective responses to both visual stimulus and imagery. Evidence is available in the study Castelo-Branco et al. 2009. This task was organized in one stationary dot and 2 moving dot conditions ('two opposing moving stimulus - 2OMS', 'four opposing moving stimulus - 4OMS') which aimed at achieving different levels of bilateral hMT+/V5 activation. In addition, an imagery condition of a square moving in 4 opposing directions ('four opposing motion

imagery - 4OMI') was included to determine the threshold used to provide feedback during the neurofeedback runs. Participants were asked to look at a fixation cross during the whole run while the sequence iterated through all condition blocks.

### Feedback threshold calculation

The thresholds used to provide feedback were determined as a function of the maximum PSC value obtained during the 4OMI condition during the localizer run. First, we use a 3-point time-window to smooth the PSC time course and minimize the impact of outliers. Then, we estimate the maximum value during the condition of interest. As a threshold for the 4OMI condition in the feedback runs, we use half of this maximum value to decrease the difficulty of obtaining positive feedback. Figure 3.3 describes the threshold calculation, where  $\mathbf{s}$  is the 3-point moving average time course,  $t$  is the index of the time point,  $\mathbf{v}$  is the PSC time course for the imagery condition,  $n$  is the total number of time points in the time course and  $\tau_+$  the threshold value.

$$\mathbf{s}_t = \frac{1}{3} \sum_{j=t}^{t+2} \mathbf{v}(j), 1 \leq t \leq n - 2;$$

$$\mathbf{S} = [s_1, s_2, \dots, s_{n-2}];$$

$$\tau_+ = \frac{1}{2} * \max[\mathbf{S}]$$

**Figure 3.3:** Equations for the calculation of the activation threshold of rewarding feedback for the condition 4OMI.

This value was also used to determine the threshold for the 2OMI condition in the feedback runs. According to Sousa et al. 2016, the ability to modulate activity based on '2 opposing moving imagery' (2OMI) task is worse (approximately half) than the modulation based on 4OMI task. In this sense, we decided to set the threshold for this condition as half of the value of  $\tau_+$ .

The negative threshold for both up-regulation conditions was set to 0 (the rationale was to inform the participants that the modulation was in the opposite direction). During the down-regulation condition, the goal was to maintain a stable BOLD signal. To inform the participants of deviations (instability of the signal, either increase or decrease), we set the positive and negative thresholds to  $\tau_+$  and  $-\tau_+$ , respectively.

### 3.2.2.2 Imagery runs

In the imagery runs, the participants were asked to perform a imagery task resembling the dot motion task performed on the localizer run. During the imagery runs, auditory cues were given to inform which task should be performed. All cues were recordings of a voice saying numbers in Portuguese indicating the number of opposing directions the participant should imagine the square moving - "zero" referred to a stationary square imagery block whilst "dois" and "quatro" referred to motion imagery with a square moving in 2 opposing directions ('two opposing motions imagery - 2OMI') and 4 opposing directions ('four opposing motion imagery - 4OMI'), respectively. Imagery runs were composed of 275 volumes divided in 25 blocks of 22 seconds.

#### **Training**

The training run is the first functional one following the localizer run. All imagery tasks are performed after the participant receives an auditory cue. Performance in this run serves as a reference value for comparison with subsequent runs.

#### **Feedback runs**

Feedback was provided in the form of 3 different vocalizations that were selected from a sub-sample by each participant to address the subjective perception of each vocalization and convey:

1. Feeling of reward
2. Neutral sound (no perception of a positive or negative reward value)
3. Feeling of punishment

The selected vocalizations were played during the runs in each TR according to the current value of mean BOLD signal achieved when compared to a positive and a negative threshold (Figure 3.4). These thresholds will be defined according to the performance of each participant in the imagery task of the localizer run.

#### **Transfer run**

The final imagery run is similar to the training run and serves as a control run to test for learning effects in feedback sessions. It also allows comparison of performance when feedback generation is present or absent.

The expectation on the transfer run is the increase in the self-regulation ability of participant when compared with the Train run. However, the limitation of the study to one NF session can be a limiting factor due to the fact the participants have a relative short time to engage in feedback-aided self-regulation.

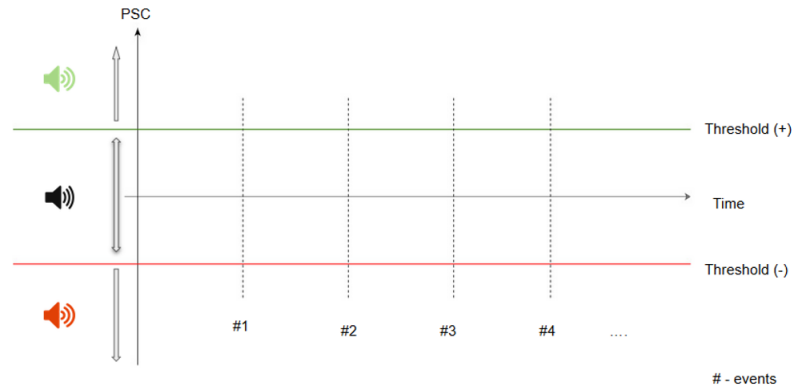


**Figure 3.4:** Feedback presentation scheme. Feedback threshold is defined in the and the events are defined as the moments when feedback is presented to the participant. The type of events will change based on the mean BOLD value (measured as a percentage of the BOLD signal variation) in the region of interest defined in bilateral area hMT+/V5.

### 3.2.3 Online fMRI processing

Turbo Brain-Voyager (Brain Innovation) was used for processing the data in real time. This software includes tools such as online 3D motion correction and alignment of functional volumes across all runs in a session. The analysis uses a recursive squares algorithm to create an online General Linear Model (GLM) (*TurboBrain-Voyager* n.d.).

#### 3.2.3.1 ROI functional definition

The selection of the region-of-interest (ROI) for feedback generation occurs during the localizer run. For this purpose, voxels corresponding to the hMT+/V5 brain area which are activated in the activation maps of the localizer run using as contrast (4OMI+2OMI>Stationary Imagery) and a statistical threshold of  $t=5$  were selected. Voxels with activations in the occipito-temporo-parietal referring to the location of the area hMT+/V5 were selected to an approximate size of 60 voxels in the functional image space.

### 3.2.4 Data analysis

Image processing and analysis were executed with both Brain Voyager QX 2.8.4 and BrainVoyager 21.2 (Brain Innovation B.V., Maastricht, The Netherlands).

Preprocessing included slice scan time correction (maximum interval between slices of 2 seconds), 3D motion detection and correction, temporal filtering (linear trend removal and temporal high pass filtering with GLM, Fourier 2 Cycles using predictors to estimate the effects of low- frequencies in a voxel's time course and remove noise)

and 3D spatial smoothing with a Gaussian filter of 6 mm. Functional data were co-registered with structural data of each participant using linear transformation and normalized to Talairach (TAL) space to allow for intersubject comparison of the results.

First-level analysis were based on a GLM using as contrast (4OMI + 2OMI > Stationary Imagery). To study the neural correlates of feedback, a GLM was designed based on regressors derived from feedback events.

In order to analyze improvements on performance during neurofeedback runs and learning effects due to neurofeedback training, the ROI-GLM statistics, both for the group and at an individual level, were compared. A NF session was labelled as successful if the t-values for the contrast (4OMI+2OMI > Stationary Imagery) showed increases between the training run and the transfer run at a statistically significant level of  $P < 0.05$ . Furthermore, the performance in self-regulation during neurofeedback runs was evaluated as positive if the t-values for the contrast (4OMI+2OMI > Stationary Imagery) for each one of the NF runs were positive.

Group analysis was performed based on a Random Effects (RFX) analysis to allow the generalization of the results to the overall population. Block protocol group analysis was conducted for the Localizer run and both NF runs to identify areas with increased activity during visual stimuli and visuospatial imagery tasks, respectively. In the Localizer run, the contrast used to generate the activation maps was (2OMS+4OMS > Stationary dot) and in the NF runs the contrast used for the same purpose was (2OMI+4OMI > Stationary Imagery). Then, an event-related protocol analysis was conducted considering separately negative and positive events for both up-regulation imagery conditions (2OMI and 4OMI) in both NF runs. The purpose of this analysis was the identification of neural correlates associated with different valence (positive or negative) feedback events during neurofeedback sessions. The software *Talairach client* was utilized to identify brain areas based on the Talairach (TAL) coordinates of the peak activations voxels as well as their corresponding Brodmann area (BA).

Lastly, an event-related averaging (ERA) analysis was conducted to analyze the hemodynamic response during the block conditions for relevant brain areas activated during event-related analysis. The spacing between feedback events was always at least 8 seconds, allowing for the calculation of the mean time course for each condition under study (Stationary Imagery, 2OMI and 4OMI). The criteria used for the selection of the brain areas was the activation during the event-related analysis and their association with literature relevant structures in the reward, salience network and auditory processing areas.



# Results

## 4.1 Group ROI analysis

### 4.1.1 ROI localization

The variability of the ROI selected across all sessions is assessed in the form of an overlap in Figure 4.1. This overlap represents the spatial consistency of activity patterns which led to the selection of the bilateral neurofeedback target area. The percentage value for each voxel represents a ratio of the number of participants with activation in the voxel and the total number of subjects in the study.

The resulting image is the ROI multi-subject cluster for the coordinates of the ROI selected as neurofeedback target during the training session for each participant with the software Turbo-BrainVoyager. The color map suggests a relatively low variability in the selection of ROI (hMT+/V5). The mean ROI size is  $3031 \text{ mm}^3$  with a standard deviation of  $417 \text{ mm}^3$ .

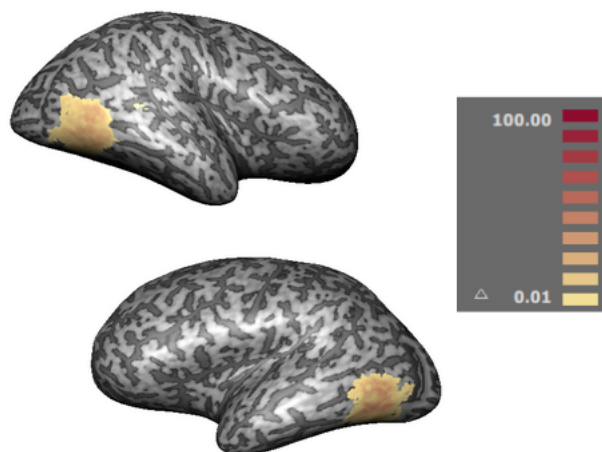


**Figure 4.1:** Group ROI cluster. The legend refers to the degree of variability between selected target regions.

### 4.1.2 Learning effects

One of the most common measures of success in NF is the comparison between modulation of the NF target during the training and transfer run. Following this logic, we determined the t-statistic for the contrast (4OMI+2OMI>Stationary Imagery) considering the NF target. Considering the overall group statistics, a decrease in the t-value is observed (not statistically significant at the  $P < 0.05$  level) (Table 4.1), suggesting that the new approach is less successful from the NF point of view than in Sousa et al. 2016.

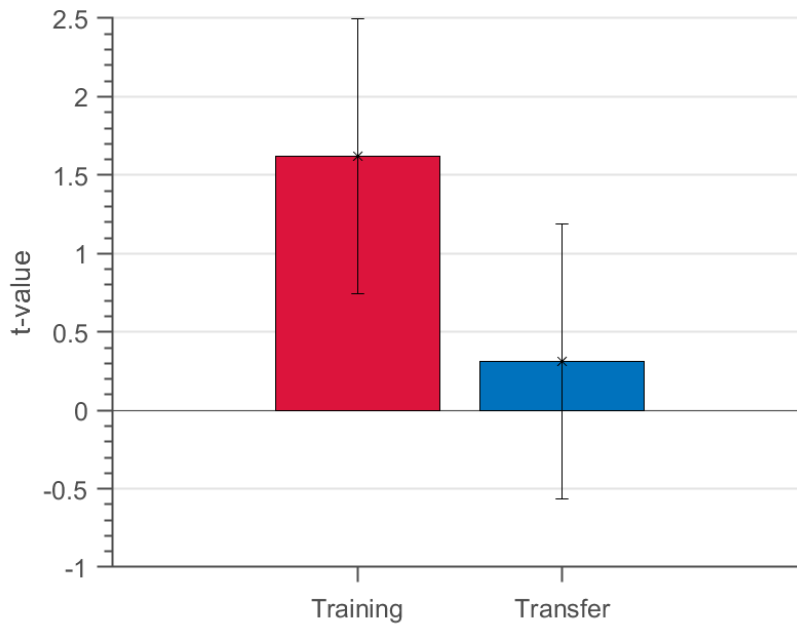


**Figure 4.2:** Group t-value statistics for the Training and Transfer runs. Values are presented as mean group value  $\pm$  standard error of mean.

<b>h</b>	<b>p-value</b>
0	0.2249

**Table 4.1:** T-test comparison for the group t-values of all participants between the Training and Transfer runs.



At the individual level, considering the ROI-GLM statistics, we observed that 4 out of 10 participants improved the self-regulation of the ROI in the transfer run (compared to the training run) (tables C.1 and C.2 in the *Appendices*). The participants identified as subjects 4,5,6 and 9 were labelled as "neurofeedback responders" (referring to participants with increases in t-statistic of the contrast of interest).

### 4.1.3 Self-regulation performance

Self-regulation performance during feedback runs is presented in the form of a comparison of the t-values for the contrast (4OMI+2OMI>Stationary Imagery). Considering the group statistics, positive t-values indicate an overall success in regulation of brain activity during the feedback sessions (Figure 4.3).

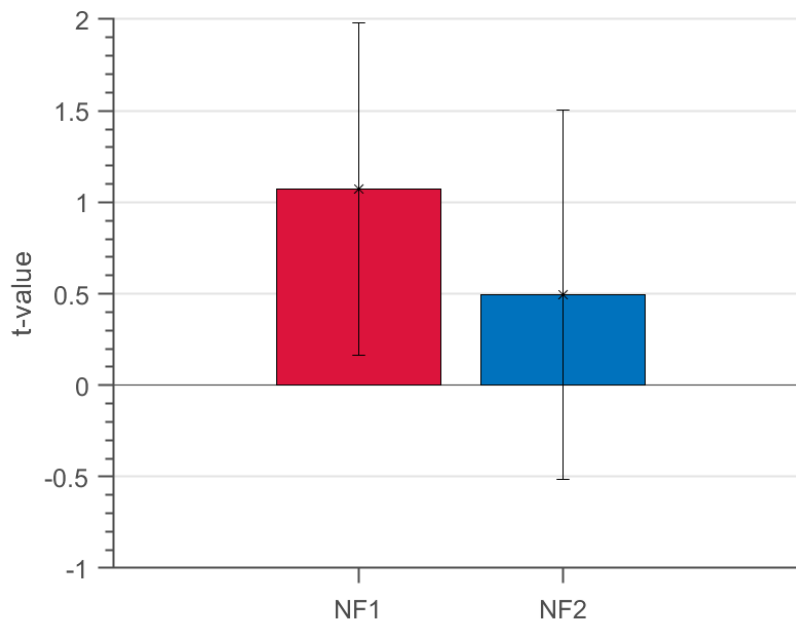


**Figure 4.3:** Group t-value statistics for the first and second NF runs. Values are presented as mean group value  $\pm$  standard error of mean.

At the individual level, ROI-GLM statistics indicate 5 participants were able to self-regulate in the first neurofeedback run (participants 1, 4, 7, 9 and 10) and 5 participants were able to self-regulate in the second neurofeedback run (participants 1, 5, 7, 9 and 10). The t-values for each individual are presented in the tables C.3 and C.4 in the *Appendices*.

## 4.2 Whole-brain group analysis

### 4.2.1 Block protocol activation maps

#### 4.2.1.1 Localizer run

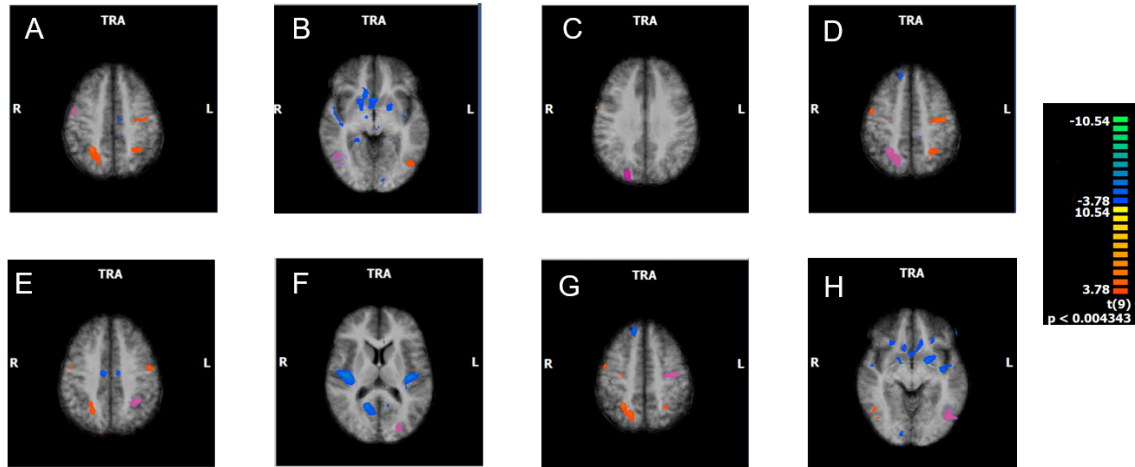
Group activation maps for the Localizer run are presented below in the form of three-dimensional surface maps (Figure 4.4) and two-dimensional transversal plane views (Figure 4.5). Both figures use as contrast the up-regulation conditions (2OMS+4OMS) versus the down-regulation (Stationary Dot).

Figure 4.4 shows activations in the neurofeedback target area (bilateral hMT+/V5), emphasizing the recruitment of this area during a visual motion task.

Figure 4.5 shows clusters of activation identified using cluster thresholding in the Brainvoyager, with a minimum threshold of 200 voxels and a  $P < 0.004343$ . The letter label used in the images refer to the brain areas and respective Brodmann Areas presented in the Table 4.2, where the coordinates of the peak voxel activated for each cluster are identified.



**Figure 4.4:** Group activation map for the Localizer run using as contrast (2OMS+4OMS>Stationary dot). The bilateral cluster shown in the activation map corresponds to the bilateral hMT+/V5 area (FDR  $q < 0.05$ )



**Figure 4.5:** Activation maps for the Localizer run using the contrast (2OMS+4OMS>Stationary dot). The areas show in purple correspond to activated resulting from cluster thresholding ( $P < 0.004343$ , cluster threshold = 200 voxels).

	Region [BA]	TAL (x,y,z)
A	Right Precentral Gyrus [BA 6]	( 48,- 1, 43)
B	Right Middle Temporal Gyrus [BA 37]	( 43,-61, -2)
C	Right Lingual Gyrus [BA 18]	( 21,-79, 31)
D	Right Superior Parietal Lobule [BA 7]	( 27,-52, 46)
E	Left Inferior Parietal Lobule [BA 40]	(-33,-46, 40)
F	Left Cuneus [BA 17]	(-24,-81, 12)
G	Left Precentral Gyrus [BA 4]	(-39,-13, 46)
H	Left Middle Occipital Gyrus [BA 37]	(-45,-67, -5)

**Table 4.2:** Peak voxels of activated cerebral regions, associated BAs and tailarach coordinates for the block analysis referring to the Localizer run ( $P < 0.004343$ , cluster minimum threshold = 200 voxels).

### 4.2.1.2 Feedback runs

Group activation maps for the Feedback runs are presented below in the form two-dimensional transversal plane views where clusters with a minimum of 200 voxels and  $P < 0.001$  (Figures 4.6 and 4.6). The contrast used to generate the maps compared the up-regulation imagery tasks (2OMI+4OMI) versus the down-regulation imagery task (Stationary Imagery).

The labels used in the images of Figure 4.6 refer to the brain areas and respective Brodmann Areas presented in the Table ??, where the coordinates of the peak voxel activated for each cluster are identified.

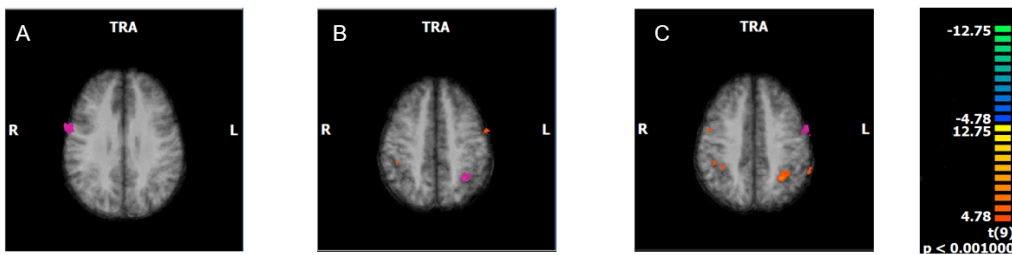


**Figure 4.6:** Activation maps representing the cluster with positive t-values using the contrast (2OMI+4OMI>Stationary imagery) for the NF runs. The areas show in purple correspond to activated resulting from cluster thresholding ( $P < 0.001$ , cluster threshold = 200 voxels).

	Region [BA]	TAL (x,y,z)
A	Right Precentral Gyrus [BA 6]	( 63, 5, 31)
B	Left Superior Parietal Lobule [BA 7]	(-30,-52, 43)
C	Left Middle Frontal Gyrus [BA 6]	(-57, 2, 40)

**Table 4.3:** Peak voxels of activated cerebral regions, associated BAs and tailarach coordinates for the block analysis referring to both NF runs ( $P < 0.001$ , cluster minimum threshold = 200 voxels).

Comparing to the study Sousa et al. 2016, the results show less brain areas with activations cluster with a minimum of 200 voxels. The divergence in the results should be associated with the more conservative type of analysis used in this study. Additionally, the activation of the Left Middle Frontal Gyrus was not reported in the above mentioned study. The literature refers the Middle Frontal gyrus plays a role in attentional control (Japee et al. 2015) which was expected in up-regulation conditions where a higher level of concentration is demanded of participants to achieve higher activation levels in the neurofeedback target area, however the lateralization of the activation is opposite to the one identified in this study.

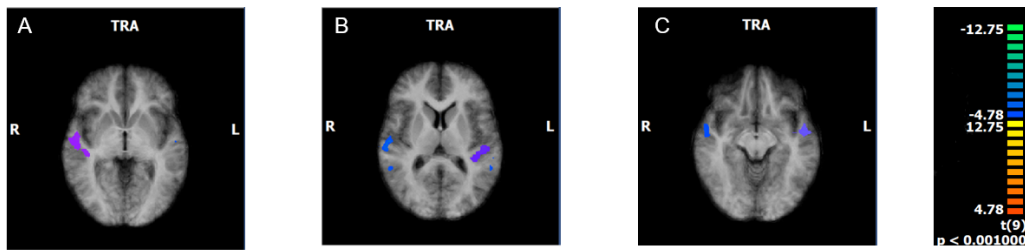


**Figure 4.7:** Activation maps representing the clusters with negative t-values peak activations in the NF runs using the contrast (2OMI+4OMI>Stationary imagery). The areas show in purple correspond to activated resulting from cluster thresholding ( $P < 0.001$ , cluster threshold = 200 voxels).

	Region [BA]	TAL (x,y,z)
A	Right Superior Temporal Gyrus [BA 22]	( 51, -7, -2)
B	Left Transverse Temporal Gyrus [BA 41]	(-42,-28, 10)
C	Left Superior Temporal Gyrus [BA 38]	(-51, -1, -5)

**Table 4.4:** Peak voxels of negative t-values for the contrast of interest. The cerebral regions, associated BAs and tailarach coordinates for the block analysis referring to both NF runs are identified. ( $P < 0.001$ , cluster minimum threshold = 200 voxels).

Peak voxels of cerebral regions with negative contrast t-values for the contrast of interest indicate higher activation levels in the Stationary Imagery condition comparing with the up-regulation conditions (2OMI and 4OMI).

## 4.2.2 Event-related protocol activation maps

In order to identify regions involved in feedback events processing, an event-related analysis based on the time points where feedback was presented (5 TR and 9 TR of each task block) was conducted. The following maps are presented according to the valence (positive or negative) of the feedback. This analysis is critical for the dissection of NF related activation of reward and "punishment" networks.

### 4.2.2.1 Positive feedback events

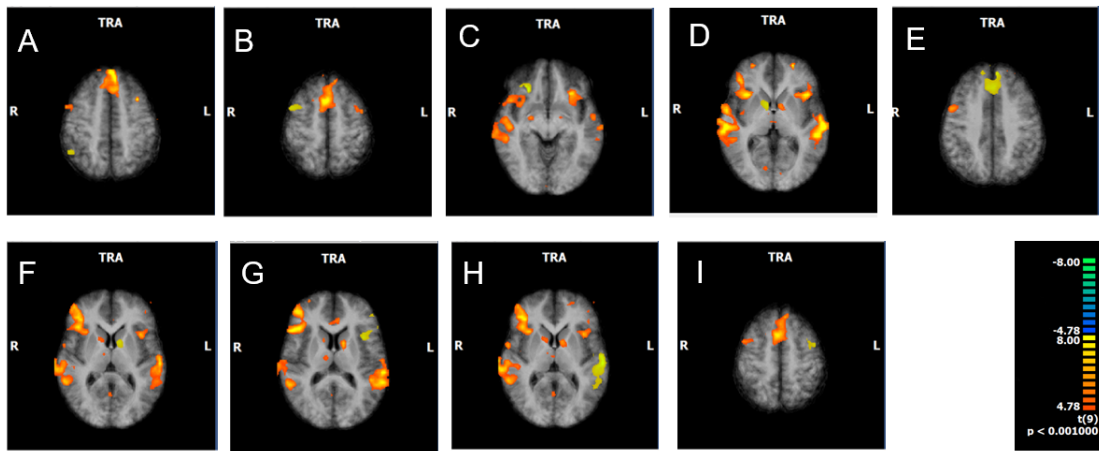


**Figure 4.8:** Activation maps representing clusters in the cerebrum for the event-related analysis referring to positive feedback concerning both NF runs. The areas show in green correspond to ROIs resulting from cluster thresholding ( $P < 0.001$ , cluster threshold = 300 voxels).

	Region [BA]	TAL (x,y,z)
A	Right Inferior Parietal Lobule [BA 40]	( 48,-53,49)
B	Right Middle Frontal Gyrus [BA 6]	(45, 5,53)
C	Right Inferior Frontal Gyrus [BA 47]	(24,29,-5)
D	Right Caudate Head	(9, 5, 1)
E	Left Superior Temporal Gyrus [BA 8]	(- 6, 41, 46)
F	Left Caudate Body	(-12,5,13)
G	Left Inferior Frontal Gyrus [BA 45]	(-57,20,19)
H	Left Superior Temporal Gyrus [BA 22]	(-60,-19, 4)
I	Left Middle Frontal Gyrus [BA 6]	(-36,- 4, 49)

**Table 4.5:** Peak voxels of activated cerebral regions, associated BAs and tailarach coordinates for the event-related analysis referring of positive feedback . Positive feedback events of both up-regulation tasks (2OMI+4OMI) in the two feedback runs were considered ( $P < 0.001$ , cluster minimum threshold = 300 voxels)

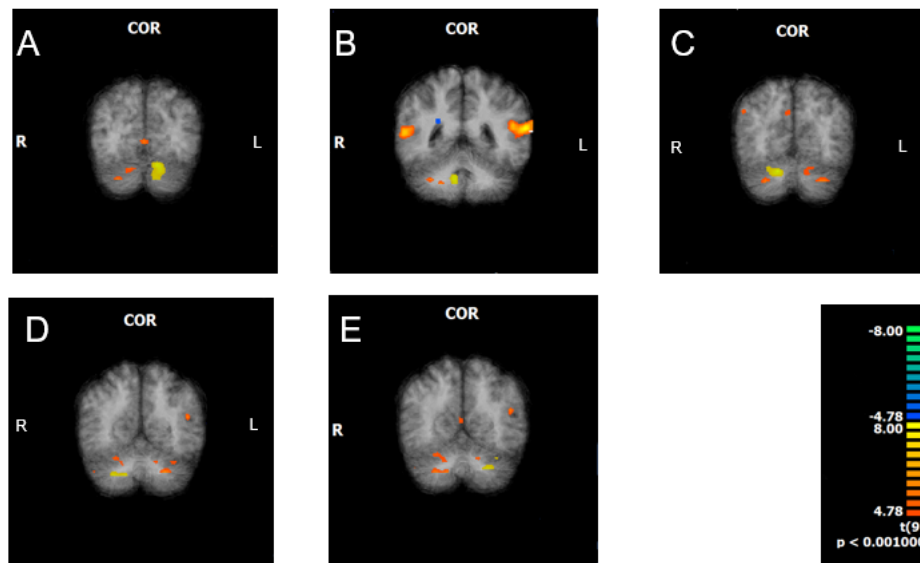


**Figure 4.9:** Activation maps representing clusters in the cerebellum for the event-related analysis referring to positive feedback concerning both NF runs. The areas show in green correspond to ROIs resulting from cluster thresholding ( $P < 0.001$ , cluster threshold = 300 voxels).

	Region	TAL (x,y,z)
A	Left Pyramis	(-12,-70,-27)
B	Right Tonsil	(6,-43,-35)
C	Right Anterior Lobe	(15,-64,-26)
D	Right Tonsil	(27,-52,-39)
E	Right Tonsil	(-24,-58,-35)

**Table 4.6:** Peak voxels of activated cerebellar regions, associated BAs and tailarach coordinates for the event-related analysis referring of positive feedback. Positive feedback events of both up-regulation tasks (2OMI+4OMI) in the two feedback runs were considered ( $P < 0.001$ , cluster minimum threshold = 300 voxels)

The voxel activations presented in Figure 4.9 associate with cerebellar structures. In the literature, there is an established relationship between the Vermis (cerebellar structure) and emotional processing, but that does not explain the preferential activation of the cerebellar structures in response to positive feedback and not negative feedback. The differential activation may present additional neural correlates of success in neurofeedback which, to the best of our knowledge, have not been identified in previous studies.

## 4.2.2.2 Negative feedback events

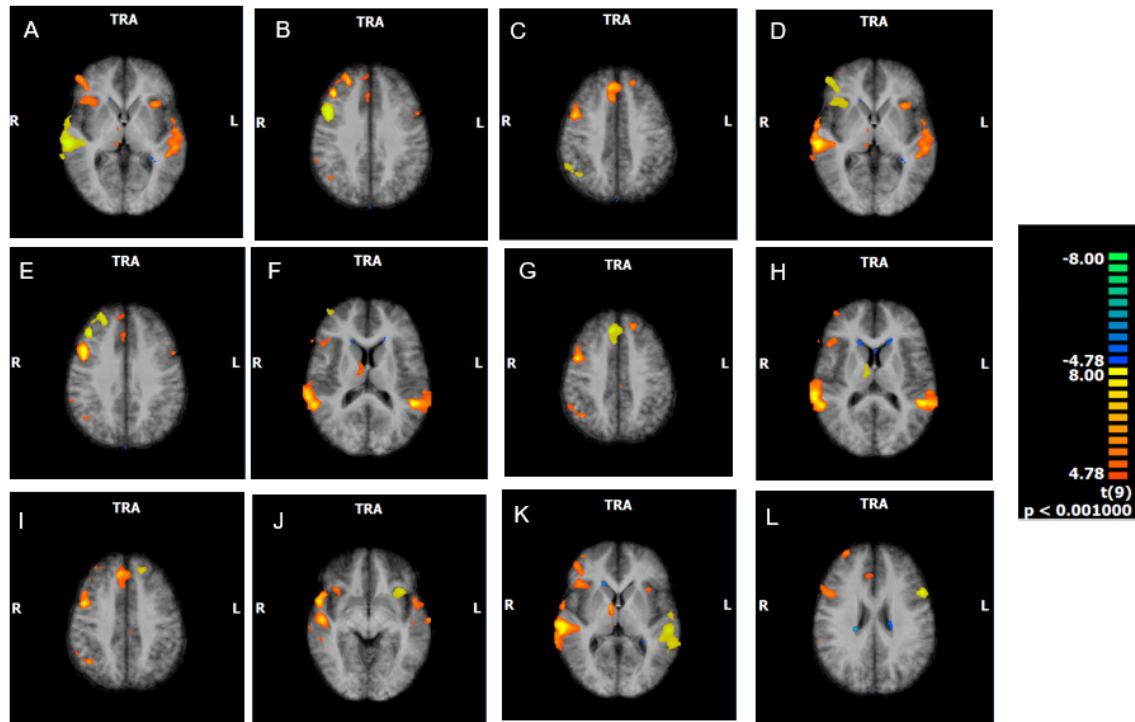


**Figure 4.10:** Activation maps for the event-related analysis referring to negative feedback events. Negative feedback events of both up-regulation tasks (2OMI+4OMI) in the two feedback runs were considered ( $P < 0.001$ , cluster minimum threshold = 300 voxels).

In addition to the reported activated areas, the results shown a deactivation on the caudate body [TAL coordinate (15,23,7)]. The result emphasizes the role of the caudate as a key structure in reward processing and operant learning, with response to both negative and positive reward-value feedback.



	<b>Region [BA]</b>	<b>TAL (x,y,z)</b>
A	Right Temporal Lobe [BA 13]	( 42,-1,-11)
B	Right Precentral Gyrus [BA 9]	(45,5,37)
C	Right Angular Gyrus [BA 39]	(39,-58,37)
D	Right Inferior Frontal Gyrus [BA 10]	(45,44, 1)
E	Right Middle Frontal Gyrus [BA 9]	(39,32,34)
F	Right Middle Frontal Gyrus [BA 10]	(39,53, 7)
G	Right Medial Frontal Gyrus [BA 8]	(3, 23,46)
H	Ventral Anterior Nucleus	(9,-4,-7)
I	Left Superior Frontal Gyrus [BA 9]	(-15,41,40)
J	Left Extra-nuclear [BA 47]	(-36, 20, -2)
K	Left Superior Temporal Gyrus [BA 13]	(-48,-43,16)
L	Left Inferior Frontal Gyrus [BA 9]	(-51,14,25)

**Table 4.7:** Peak voxels of activated cerebral regions, associated BAs and tailarach coordinates for the event-related analysis referring to negative feedback. Negative feedback events of both up-regulation tasks (2OMI+4OMI) in the two feedback runs were considered ( $P < 0.001$ , cluster minimum threshold = 300 voxels).

### 4.2.3 Event-related averaging time course analysis

An event-related averaging analysis was performed to analyze the hemodynamic response profile of the block conditions in a selective group of ROIs following a stimulus (both the auditory cue and the feedback). The mean time course for each condition resulted from the averaging all peri-stimulus time course segments corresponding to the same block condition. The mean time courses of the three different feedback tasks (Stationary Imagery, 2OMI and 4OMI) are superimposed in the figures to allow for a relative comparison of the response profiles.

The ROIs were chosen based on the differential activated structures in the event-related protocol activation maps and their association in the literature with a prevalent role in feedback processing. This include:

- The Auditory Cortex (Brodmann area 22)
- Caudate
- Thalamus
- Insula

### 4.2.3.1 Primary Auditory Cortex (Brodmann Area 22)

The involvement of the auditory cortex in the auditory processing of the stimuli is emphasized by the similar average response profiles for all imagery tasks. Figure 4.11 represents the ERA for the volume time course resulting from event-related protocol of positive feedback events.

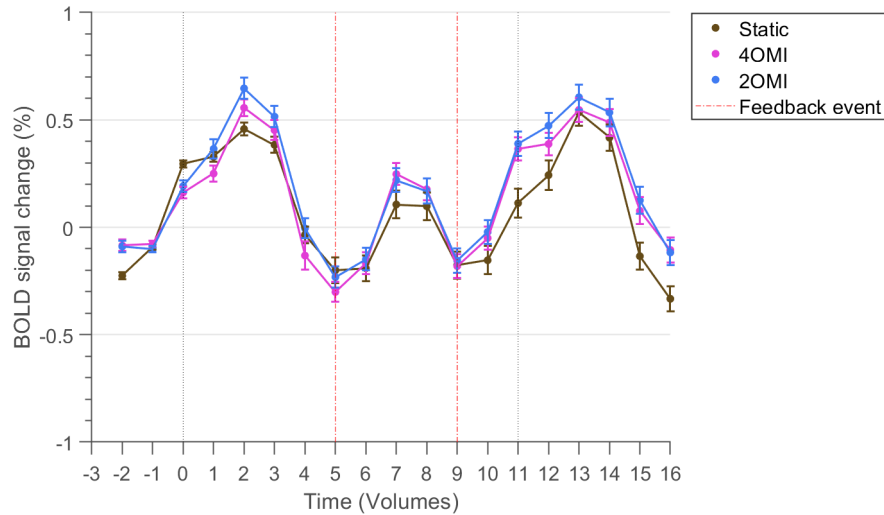


**Figure 4.11:** ERA of the three imagery tasks ROI with Tailarach coordinates (-60,-19,4) for both neurofeedback runs. The purple curve represents the ERA of the condition **4OMI**, the blue curve represents the ERA of condition **2OMI** and the brown curve represents the ERA of the condition **Stationary Imagery**. Black vertical lines represent the volume where the task block is initiated, following the presentation of the auditory cue (TR=0) and the end of the task block (TR=11).

The ERA in Figure 4.11 indicates, as expected, the BOLD signal variation in the primary auditory cortex is independent of task or auditory stimulus across all tasks. The increase in the activity levels in the ROI following the task cue is higher when compared with the first feedback event. This difference ought to be associated with the fact the second feedback event occurs 2 volumes (TRs) before the generation of the auditory cue, leading to an accumulation of the effects of both auditory stimuli.

### 4.2.3.2 Caudate

In the previous section, the caudate activated in response to a positive feedback event (caudate head) and decreased in activation in response to a negative feedback event (caudate body).

Figure 4.12 represents the ERA of the caudate head for the volume time course resulting from event-related protocol of positive feedback events. Figure 4.13 represents the ERA of the caudate body for the volume time course resulting from event-related protocol of negative feedback events. The increase in caudate BOLD signal following the first positive feedback event contrasts with the decrease following the first negative feedback event. Furthermore, Figure 4.12 suggests the caudate activation is dependent on the task, with distinct levels of activation depending on the type of task.

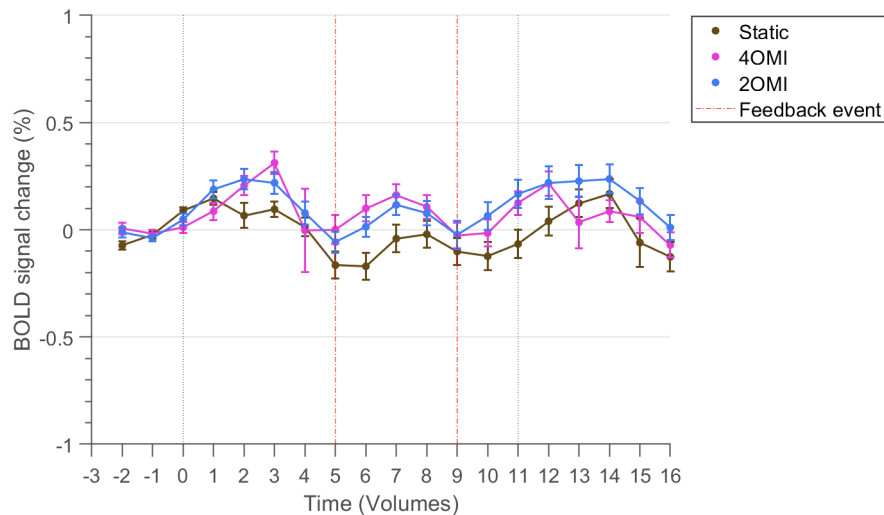


**Figure 4.12:** ERA of the three imagery tasks ROI with Tailarach coordinates (9,5,1) for both neurofeedback runs. The purple curve represents the ERA of the condition **4OMI**, the blue curve represents the ERA of condition **2OMI** and the brown curve represents the ERA of the condition **Stationary Imagery**. Black vertical lines represent the volume where the task block is initiated, following the presentation of the auditory cue (TR=0) and the end of the task block (TR=11).

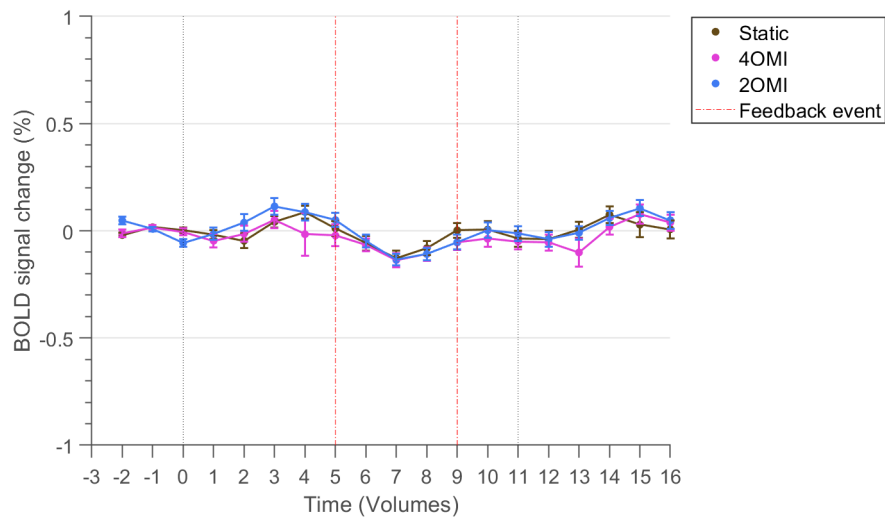


**Figure 4.13:** ERA of the three imagery tasks ROI with Tailarach coordinates (9,5,1) for both neurofeedback runs. The purple curve represents the ERA of the condition **4OMI**, the blue curve represents the ERA of condition **2OMI** and the brown curve represents the ERA of the condition **Stationary Imagery**. Black vertical lines represent the volume where the task block is initiated, following the presentation of the auditory cue (TR=0) and the end of the task block (TR=11).

### 4.2.3.3 Thalamus

The activation of the ventral anterior nucleus is dependent of the valence of the feedback, occurring only in response to negative feedback. The anterior nuclei of the thalamus have been reported to be involved in functions of alertness. Figure 4.14 represents the ERA for the volume time course resulting from event-related protocol of negative feedback events.

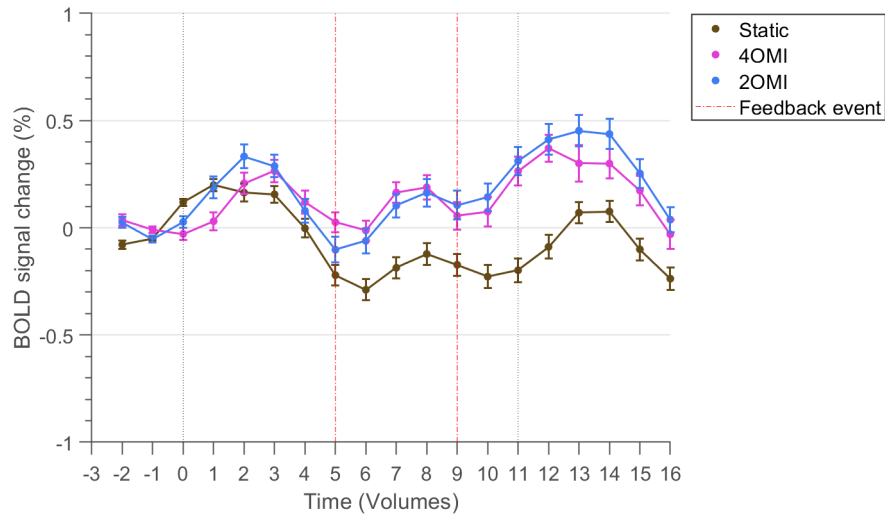


**Figure 4.14:** ERA of the three imagery tasks in the the ventral anterior nucleus [TAL (9,-4,-7)] for both neurofeedback runs concerning the event-related negative feedback volume time course. The purple curve represents the ERA of the condition **4OMI**, the blue curve represents the ERA of condition **2OMI** and the brown curve represents the ERA of the condition **Stationary Imagery**. Black vertical lines represent the volume where the task block is initiated, following the presentation of the auditory cue (TR=0) and the end of the task block (TR=11).

The ERA in Figure 4.14 suggests the BOLD signal variation in the thalamus reflects the needed level of engagement with the task, with the different conditions showing similar level of amplitude variation but with distinct base activity levels following the first feedback event (up-regulation imagery tasks shown with higher activity levels comparing with Stationary imagery).

#### 4.2.3.4 Insula

The insula is a key brain area of the salience network, which is activated in response to negative feedback. Figure 4.15 represents the ERA for the volume time course resulting from event-related protocol of negative feedback events.

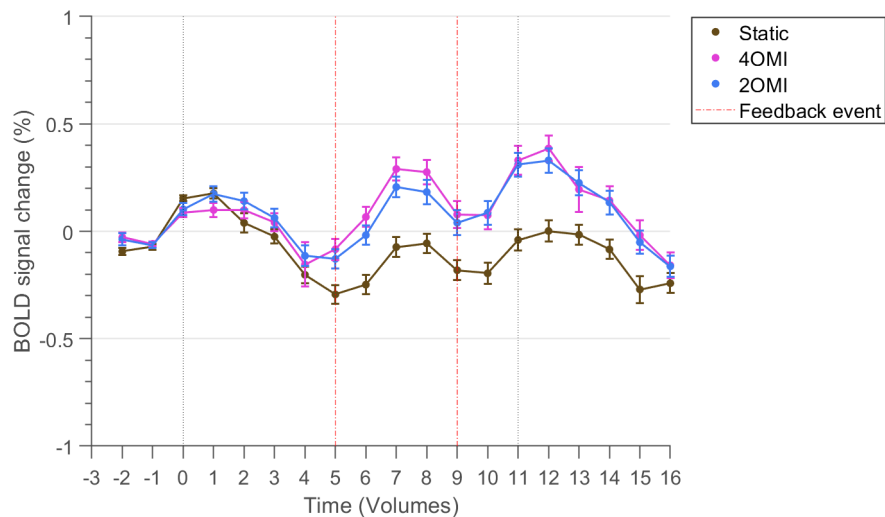


**Figure 4.15:** ERA of both neurofeedback runs in the the anterior nucleus with [TAL (36,21,4)] The purple curve represents the ERA of the condition **4OMI**, the blue curve represents the ERA of condition **2OMI** and the brown curve represents the ERA of the condition **Stationary Imagery**. Black vertical lines represent the volume where the task block is initiated, following the presentation of the auditory cue (TR=0) and the end of the task block (TR=11).

The ERA in Figure 4.15 appears to indicate the BOLD signal variation in the insula reflects the needed level of engagement with the task, with the different conditions showing similar level of amplitude variation but with distinct base activity levels following the first feedback event (up-regulation imagery tasks shown with higher activity levels comapring with Stationary imagery).





# Discussion

## Contributions to the state of the art

Functional and anatomical MRI data were acquired from ten healthy patients to explore the neural correlates of feedback in relation to the reward and salience networks and the putative association with individual variations associated to the success of the training. There has been some interest on the neural correlates of feedback processing and success in neurofeedback sessions independent of task and neurofeedback target, namely a study focusing solely on visual feedback paradigms (Skottnik et al. 2019). In this study, the experimental protocol adds value to the state of the art by analyzing whole-brain activations concurrent with specific feedback events by using emotional human vocalization auditory positive and negative feedback. Equipped with such an event related approach, the experimental design enabled to specifically identify neural correlates of reward and aversion during feedback runs, making no assumptions for the selection of ROIs before data acquisition.. The overall results serve as a exploratory analysis to identify biomarkers on positive and negative feedback processing.

The percentage of successful neuromodulators in the present work was 40%, which is in accordance with reported estimated percentages of success across a variety of neurofeedback studies according to the review Alkoby et al. 2018. The implementation of a tailored neurofeedback paradigm did not result in the increase of "successful responders" as expected, which is inclusively reduced when comparing to the results in the study Sousa et al. 2016. The motivation for the adaptation of the existing experimental protocol derived from the need to further understand the neural correlates of success and failure associated with feedback events processing in order to optimize and adapt NF protocols to maximize the participants' performance and learning. However, the implementation of the new protocol failed its purpose of enhancing performance during the session. The overall decreased frequency of feedback may have led to a decrease on attention in the task and, consequently, an increase in the relative number of negative feedback events. This work does therefore provide important insight into the need to optimize frequency of feedback in NF protocols.

Also, the fact that this study utilized solely one feedback session per participant may have limited the results, which is supported by the fact that experienced participants received more positive feedback during NF runs than unexperienced participants (data available in the Appendices). Nevertheless, performance in the transfer runs declined across both groups of participants (both experienced and unexperienced), which indicate frustration and fatigue may have played a role. This effect can be confirmed by the group trend in t-values in the feedback runs (Figure 4.3). This work does therefore provide important insight into the need to optimize frequency of feedback in NF protocols.

The parametric activation paradigm used did not allow for the direct comparison between reward and aversion feedback processing due to the lack of positive and negative events in some feedback runs in the subjects, which would require excluding participants from the analysis. Moreover the neural correlates of positive feedback and punishment are known to be non-overlapping. In the future, the increase of the sample size of participants will allow the comparison of results between parametric activation tasks with the neural correlates of positive and negative feedback identified in the present work.

In addition, neutral feedback events should also be considered to understand how it is perceived by the participants and their role in the success of self-regulation. In this study they were not considered for analysis due to time constraints for the realization of the analysis. The aim of the study was centered on the duality of networks between punishing and rewarding feedback, using the neutral events solely to better inform the participant of the activation level in the neurofeedback target (hMT+/V5) during the tasks.

### **Auditory Processing areas**

Activations across different auditory processing areas were verified. The peak voxel activations were identified as the BA 45, 47 and 22. The BA 47 is associated with processing of non-spatial sound information (Arnott et al. 2004) and BA 45 is associated with phonological processing (Heim et al. 2003), both specific aspects of auditory processing. On the other hand, BA 22 refers to the primary auditory cortex, which is involved in the processing of all auditory stimuli (Moerel, De Martino, and Formisano 2014).

The activations in the several auditory areas in response to both positive and negative feedback were expected to occur since these relate to the auditory processing of the information. The difference in peak voxel activations between the two feedback types are not significant for the interpretation of differential activated regions in the auditory cortex since the clusters engulf the bilateral auditory cortex (evident in

the bilateral clusters occipito-temporo-parietal area on the activation maps A,D,F,H and K from Figure 4.10 and B,F,G and H of Figure 4.8).

### **Reward-value independent activations**

Activations non-auditory related were verified independent of reward-value of the feedback. The involvement of BA 47 in conflict management and processing changes in the reward value of new information may be the reason for its activation (Rogers et al. 1999). Activations in BA 8 for both feedback types independent of valence (positive and negative) supports the involvement of processes of uncertainty mediation following the feedback stimulus (Volz, Schubotz, and Von Cramon 2004). Activations in the angular gyrus and the right inferior parietal lobule may refer to their role in commanding attention during the onset of salient new information, such as feedback (Singh-Curry and Husain 2009).

### **Reward-value dependent activations**

Activations in different neural structures were verified based on the type of feedback event. Activations in central regions on the dopamine mesolimbic pathway were quite evident, such as the striatum (caudate head and body) in response to rewarding feedback. The relevance of the striatum in the processing of feedback with explicit emotional valence is further emphasized by the deactivation following “punishing” feedback, as it is described in the Figure 4.13, which suggests a confirmation of the results of Skottnik et al. 2019.

The activation of the right Middle Frontal Gyrus may play an important role in reorienting attention between the exogenous environmental stimuli (feedback event) and the mental strategy in use (Japee et al. 2015).

Interestingly, results point to an exclusive involvement of cerebellar structures in the processing of positive feedback. The cerebellum is involved in error correction regarding motor control as well as emotional processing (Snow, Stoesz, and Anderson 2014). The activation of a variety of cerebellar structures in contrast with negative feedback was not anticipated and is not supported by the literature to our knowledge. Activations associated with negative valence feedback are mainly involved in alertness and arousal processes evoked by conflict adaptation (thalamus), as well as management and monitoring of sub-goals while maintaining information in working memory (BA 10) (Ramnani and Owen 2004). In addition, activations in the insular cortex area (BA 13) is consistent with reports on the importance of this area on risk-taking decisions and response to punishment. (Paulus et al. 2003).

As expected, these results indicate distinct regions that may serve as negative performance indicators during the activation tasks in contrast to positive performance indicators who are identifiable within the main classical structures of the reward

processing system.

## 6

# Conclusions

In the present work, we have found evidence of differential neural correlates for rewarding and aversive feedback during a neurofeedback experiment. The association between success and patterns of activation within the reward system may serve as the basis for the usage of such neural markers as indicators that can be used to optimize feedback training and personalize the level of challenge for neuromodulation to each individual's specific psychological characteristics.

Subsequent studies ought to focus on confirming results for less common feedback interface alternatives (such as haptic and electroactile). Similar results would confer higher credibility to the connections between these biomarkers and success in the overall neurofeedback design framework.

The literature on neurofeedback mostly focuses on visual feedback neurofeedback experiments. The confirmation of the involvement of similar brain areas in feedback processing for auditory display with explicit positive and negative emotional valence, provides a new way to link neurofeedback with interfaces exhibiting a cued valence. It would be of utmost interest to study the functional connectivity between the identified biomarkers of neurofeedback success. A measure of the number of effective connections in neurofeedback runs can be performed for example using the multivariate Granger Causality Matlab Toolbox, pairing ROIs previously identified in the RFX analysis to the causality of activations. This information may have value to inform on the relationship between the psychological factors and activations of specific brain networks, related to biomarkers that may be critical in predicting success during feedback training.

Ultimately, this research is directed to contribute to the the definition of adaptive neurofeedback paradigms, by discovering patterns related to success criteria which can be used to define neuroimaging biomarkers for NF success.









# Appendices



# A

## Pilot Studies

Pilot studies were performed to validate the identification of activity in reward-related brain structures and optimize the design of the experiment to the participants feedback about stimulus presentation, auditory cues, feedback sounds and length of the experiment. All modifications to the overall experiment design aimed at increasing subsequent participants task engagement and motivation during the session.

### A.1 First Pilot study

The goal of the first pilot study was to analyze the cortical activation of cortical areas that are included in the reward system and analyze if such activations are time-dependent of the feedback generation during NF runs. At this stage, the session organization model only contained a localizer run, a no-feedback imagery run and a feedback run. In terms of feedback sounds, the participant did not choose personalized vocalizations and was presented with generic vocalizations "Up", "Null", "Down". The feedback of the participant about the vocalizations and its negative effect on the overall engagement on the task motivated the personalization of auditory feedback achieved with the pre-session questionnaire.

The results presented in Figure A.1 were obtained using a different software for image processing and analysis called SPM Version 12 (Statistical Parametric Mapping, Functional Imaging Laboratory). Image processing occurred using the same parameters for preprocessing as the participants included in the results of the study. The toolbox AAL (Automated Anatomical Labelling, Neurofunctional Imaging Group) was used as an atlas to identify the anatomical brain structures associated with the voxels activated using as contrast  $40MI+20MI>Stationary\ Imagery$ . The AAL toolbox uses the reference space MNI (Montreal Neurological Institute) instead of TAL to associate activated voxels with anatomical locations.

The results identify activated voxels in two brain areas associated with error prediction: the orbitofrontal cortex and the cingulum. Both areas are connected to main

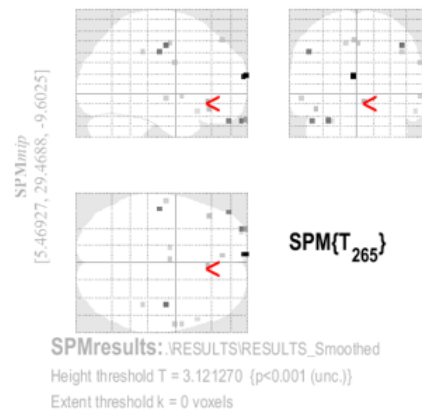


**Figure A.1:** Activation maps resulting from whole brain event-related analysis (SPM12) shows activated voxels in areas such as the orbitofrontal cortex ( $T=3.94$ ,  $p<0.001$ ) and the cingulum ( $T=3.35$ ,  $p<0.001$ ). Anatomical identification was performed based on MNI coordinates and the AAL toolbox.

reward-related brain areas and have been linked to reward prediction (Stalnaker et al. 2018; Bubb, Metzler-Baddeley, and Aggleton 2018).

## A.2 Second Pilot Study

The second pilot study served the purpose of optimizing length of experiment and evaluating the perception of the auditory cues used in imagery runs. Auditory cues were vocalizations of letters "A", "B" and "C" which respectively identified the tasks "stationary square imagery", "motion imagery in 2 opposing directions" and "motion imagery in 4 opposing directions". The participant's feedback during the session allowed the definition of the definitive session organization of the runs as well as the modification of auditory cues to vocalizations identifying the number of opposing directions for each imagery task.

# B

## Participants details

Participants List				
Participant ID	Gender	Age	Laterality	rtfMRI/NF Experience
1	Female	23	Right-handed	None
2	Female	23	Right-handed	None
3	Male	28	Right-handed	None
4	Female	25	Right-handed	None
5	Female	19	Right-handed	None
6	Female	23	Left-handed	None
7	Male	35	Right-handed	rtfMRI + NF
8	Male	24	Right-handed	None
9	Male	25	Right-handed	None
10	Male	35	Right-handed	rtfMRI + NF

**Table B.1:** Participants details. Participants are described according to gender, age, dominant hand (laterality) and their previous experience with rtfMRI or NF sessions.

# C

## Individual ROI-GLM Statistics

### C.1 Training run

Training run		
Subject	t-value	p-value
1	4.3207	0.000022
2	2.9297	0.003692
3	3.0628	0.002427
4	-1.6529	0.099583
5	0.6399	0.5228
6	-3.7498	0.000218
7	3.2972	0.001112
8	3.4739	0.000600
9	-0.4423	0.658647
10	4.3284	0.000021

**Table C.1:** Individual ROI-GLM statistics for each participant for the training run. The t-values and p-values presented refer the NF target and the contrast (4OMI+2OMI > Stationary Imagery)

## C.2 Transfer run

Transfer run		
Subject	t-value	p-value
1	-2.0260	0.043774
2	-2.9383	0.0035942
3	2.7737	0.005941
4	1.8796	0.0614783
5	1.06340	0.288331
6	-2.3086	0.021756
7	1.9630	0.050713
8	0.1548	0.877340
9	0.4520	0.651636
10	2.0947	0.037155

**Table C.2:** Individual ROI-GLM statistics for each participant for the transfer run. The t-values and p-values presented refer the NF target and the contrast (4OMI+2OMI >Stationary Imagery)



### C.3 First neurofeedback run

NF #1		
Subject	t-value	p-value
1	3.2105	0.0015
2	-2.4434	0.0152
3	-0.7704	0.4418
4	1.9764	0.0492
5	-1.4368	0.1519591
6	-0.3554	0.722565
7	3.3279	0.001000
8	-2.1121	0.035650
9	3.2806	0.001177
10	6.0418	$5.208958 \times 10^{-9}$

**Table C.3:** Individual ROI-GLM statistics for each participant for the first neurofeedback run. The t-values and p-values presented refer the NF target and the contrast (4OMI+2OMI>Stationary Imagery)

## C.4 Second neurofeedback run

NF #2		
Subject	t-value	p-value
1	1.5355	0.1258627
2	-2.3477	0.019662
3	-1.8904	0.059817
4	-2.0503	0.041417
5	0.6686	0.504371
6	-0.8041	0.422055
7	2.7951	0.005576
8	-3.4275	0.000707
9	4.0070	0.000080
10	6.4684	$4.832791 \times 10^{-10}$

**Table C.4:** Individual ROI-GLM statistics for each participant for the second neurofeedback run. The t-values and p-values presented refer the NF target and the contrast (4OMI+2OMI>Stationary Imagery)

# Bibliography

- Alexander, Garrett E. and Michael D. Crutcher (1990). “Functional architecture of basal ganglia circuits: neural substrates of parallel processing”. In: *Trends in Neurosciences* 13.7, pp. 266–271. ISSN: 01662236. DOI: 10.1016/0166-2236(90)90107-L. URL: <https://linkinghub.elsevier.com/retrieve/pii/016622369090107L>.
- Alkoby, O. et al. (2018). “Can We Predict Who Will Respond to Neurofeedback? A Review of the Inefficacy Problem and Existing Predictors for Successful EEG Neurofeedback Learning”. In: *Neuroscience* 378.2017, pp. 155–164. ISSN: 18737544. DOI: 10.1016/j.neuroscience.2016.12.050. URL: <http://dx.doi.org/10.1016/j.neuroscience.2016.12.050>.
- Araki, Masasuke, Patrick L. McGeer, and Hiroshi Kimura (1988). “The efferent projections of the rat lateral habenular nucleus revealed by the PHA-L anterograde tracing method”. In: *Brain Research* 441.1-2, pp. 319–330. ISSN: 00068993. DOI: 10.1016/0006-8993(88)91410-2.
- Arnott, Stephen R. et al. (2004). “Assessing the auditory dual-pathway model in humans”. In: *NeuroImage* 22.1, pp. 401–408. ISSN: 10538119. DOI: 10.1016/j.neuroimage.2004.01.014.
- Barth, Markus and Benedikt A. Poser (2011). “Advances in high-field bold fmri”. In: *Materials* 4.11, pp. 1941–1955. ISSN: 19961944. DOI: 10.3390/ma4111941.
- Beres, Anna M. (2017). “Time is of the Essence: A Review of Electroencephalography (EEG) and Event-Related Brain Potentials (ERPs) in Language Research”. In: *Applied Psychophysiology Biofeedback* 42.4, pp. 247–255. ISSN: 10900586. DOI: 10.1007/s10484-017-9371-3.
- Bevan, M.D., A.D. Smith, and J.P. Bolam (1996). “The substantia nigra as a site of synaptic integration of functionally diverse information arising from the ventral pallidum and the globus pallidus in the rat”. In: *Neuroscience* 75.1, pp. 5–12. ISSN: 03064522. DOI: 10.1016/0306-4522(96)00377-6. URL: <https://linkinghub.elsevier.com/retrieve/pii/0306452296003776>.
- Breteler, Marinus H.M. et al. (2010). “Improvements in spelling after QEEG-based neurofeedback in dyslexia: A randomized controlled treatment study”. In: *Ap-*

- plied Psychophysiology Biofeedback* 35.1, pp. 5–11. ISSN: 10900586. DOI: 10.1007/s10484-009-9105-2.
- Brown, R.W., Y.N. Cheng, and E.M Haacke (2018). *Magnetic Resonance Imaging: Physical Principles and Sequence Design*. John Wiley & Sons Inc. ISBN: 978-0-471-72085-0.
- Bubb, Emma J., Claudia Metzler-Baddeley, and John P. Aggleton (2018). “The cingulum bundle: Anatomy, function, and dysfunction”. In: *Neuroscience and Biobehavioral Reviews* 92.2010, pp. 104–127. ISSN: 18737528. DOI: 10.1016/j.neubiorev.2018.05.008. URL: <https://doi.org/10.1016/j.neubiorev.2018.05.008>.
- Caria, Andrea et al. (2010). “Volitional control of anterior insula activity modulates the response to aversive stimuli. A real-time functional magnetic resonance imaging study”. In: *Biological Psychiatry* 68.5, pp. 425–432. ISSN: 00063223. DOI: 10.1016/j.biopsych.2010.04.020. URL: <http://dx.doi.org/10.1016/j.biopsych.2010.04.020>.
- Castelo-Branco, Miguel et al. (2009). “Type of featural attention differentially modulates hMT+ responses to illusory motion aftereffects”. In: *Journal of Neurophysiology* 102.5, pp. 3016–3025. ISSN: 00223077. DOI: 10.1152/jn.90812.2008.
- Chesworth, Rose and Laura Corbit (2017). “The Contribution of the Amygdala to Reward-Related Learning and Extinction”. In: *The Amygdala - Where Emotions Shape Perception, Learning and Memories*. Vol. i. tourism. InTech, p. 13. DOI: 10.5772/67831.
- Cowen, Alan S. et al. (2018). “Mapping 24 emotions conveyed by brief human vocalization”. In: *American Psychologist* January 2019. ISSN: 0003066X. DOI: 10.1037/amp0000399.
- Cox, Robert W, Andrzej Jesmanowicz, and James S Hyde (1995). “Real-Time Functional Magnetic Resonance Imaging”. In: *Magnetic Resonance in Medicine* 33.2, pp. 230–236. ISSN: 07403194. DOI: 10.1002/mrm.1910330213. URL: <http://doi.wiley.com/10.1002/mrm.1910330213>.
- Dale, A. M. and R. L. Buckner (1997). “Selective averaging of individual trials using fMRI”. In: *NeuroImage* 5.4 PART II, pp. 329–340. ISSN: 10538119.
- Dewiputri, Wan Ilma and Tibor Auer (2013). “Functional magnetic resonance imaging (fMRI) neurofeedback: Implementations and applications”. In: *Malaysian Journal of Medical Sciences* 20.5, pp. 5–15. ISSN: 1394195X.
- Elbert, Thomas et al. (1980). “Biofeedback of slow cortical potentials. I”. In: *Electroencephalography and Clinical Neurophysiology* 48.3, pp. 293–301. ISSN: 00134694. DOI: 10.1016/0013-4694(80)90265-5.

- Gattass, Ricardo et al. (2005). “Cortical visual areas in monkeys: Location, topography, connections, columns, plasticity and cortical dynamics”. In: *Philosophical Transactions of the Royal Society B: Biological Sciences* 360.1456, pp. 709–731. ISSN: 09628436. DOI: 10.1098/rstb.2005.1629.
- Gauthier, Jeffrey L. and David W. Tank (2018). “A Dedicated Population for Reward Coding in the Hippocampus”. In: *Neuron* 99.1, pp. 179–193. ISSN: 10974199. DOI: 10.1016/j.neuron.2018.06.008. URL: <https://doi.org/10.1016/j.neuron.2018.06.008>.
- Gevensleben, Holger et al. (2014). “Neurofeedback of slow cortical potentials: Neural mechanisms and feasibility of a placebo-controlled design in healthy adults”. In: *Frontiers in Human Neuroscience* 8.DEC, pp. 1–13. ISSN: 16625161. DOI: 10.3389/fnhum.2014.00990.
- Gray, Sarah N. (2017). “An Overview of the Use of Neurofeedback Biofeedback for the Treatment of Symptoms of Traumatic Brain Injury in Military and Civilian Populations”. In: *Medical Acupuncture* 29.4, pp. 215–219. ISSN: 19336594. DOI: 10.1089/acu.2017.1220.
- Gremel, C. M. and D. M. Lovinger (2017). “Associative and sensorimotor cortico-basal ganglia circuit roles in effects of abused drugs”. In: *Genes, Brain and Behavior* 16.1, pp. 71–85. ISSN: 1601183X. DOI: 10.1111/gbb.12309.
- Haber, Suzanne N. and Brian Knutson (2010). “The reward circuit: Linking primate anatomy and human imaging”. In: *Neuropsychopharmacology* 35.1, pp. 4–26. ISSN: 0893133X. DOI: 10.1038/npp.2009.129. URL: <http://dx.doi.org/10.1038/npp.2009.129>.
- Hassan, Muhammad Abul et al. (2015). “The mechanism of neurofeedback training for treatment of central neuropathic pain in paraplegia: A pilot study”. In: *BMC Neurology* 15.1, pp. 1–13. ISSN: 14712377. DOI: 10.1186/s12883-015-0445-7. URL: <http://dx.doi.org/10.1186/s12883-015-0445-7>.
- Hauser, Tobias U., Eran Eldar, and Raymond J. Dolan (2017). “Separate mesocortical and mesolimbic pathways encode effort and reward learning signals”. In: *Proceedings of the National Academy of Sciences of the United States of America* 114.35, E7395–E7404. ISSN: 10916490. DOI: 10.1073/pnas.1705643114.
- Heim, St et al. (2003). “Phonological processing during language production: fMRI evidence for a shared production-comprehension network”. In: *Cognitive Brain Research* 16.2, pp. 285–296. ISSN: 09266410. DOI: 10.1016/S0926-6410(02)00284-7.
- Hu, Hailan (2016). “Reward and Aversion”. In: *Annual Review of Neuroscience* 39.1, pp. 297–324. ISSN: 0147-006X. DOI: 10.1146/annurev-neuro-070815-014106.

- Japee, Shruti et al. (2015). “A role of right middle frontal gyrus in reorienting of attention: A case study”. In: *Frontiers in Systems Neuroscience* 9.MAR, pp. 1–16. ISSN: 16625137. DOI: 10.3389/fnsys.2015.00023.
- Jiang, Yang, Reza Abiri, and Xiaopeng Zhao (2017). “Tuning up the old brain with new tricks: Attention training via neurofeedback”. In: *Frontiers in Aging Neuroscience* 9.MAR, pp. 1–9. ISSN: 16634365. DOI: 10.3389/fnagi.2017.00052.
- Kadosh, Kathrin Cohen and Graham Staunton (2018). “A systematic review of the psychological factors that influence neurofeedback learning outcomes”. In: *NeuroImage*. ISSN: 10959572. DOI: 10.1016/j.neuroimage.2018.10.021. URL: <https://doi.org/10.1016/j.neuroimage.2018.10.021>.
- Kobayashi, Yasushi and Ken Ichi Okada (2007). “Reward prediction error computation in the pedunculopontine tegmental nucleus neurons”. In: *Annals of the New York Academy of Sciences* 1104, pp. 310–323. ISSN: 17496632. DOI: 10.1196/annals.1390.003.
- Kouijzer, Mirjam E J et al. (2013). “Is EEG-biofeedback an effective treatment in autism spectrum disorders? A randomized controlled trial”. In: *Applied Psychophysiology Biofeedback* 38.1, pp. 17–28. ISSN: 10900586. DOI: 10.1007/s10484-012-9204-3.
- Koush, Yury et al. (2013). “Connectivity-based neurofeedback: Dynamic causal modeling for real-time fMRI”. In: *NeuroImage* 81, pp. 422–430. ISSN: 10538119. DOI: 10.1016/j.neuroimage.2013.05.010. URL: <http://dx.doi.org/10.1016/j.neuroimage.2013.05.010>.
- Latchaw, R.E., J. Kucharczyk, and M.E. Moseley (2005). *Imaging of the Nervous System: Diagnostic and Therapeutic Applications*. vol. 1. Elsevier Mosby. ISBN: 9780323011839.
- LeGates, Tara A. et al. (2018). “Reward behaviour is regulated by the strength of hippocampus–nucleus accumbens synapses”. In: *Nature* 564.7735, pp. 258–262. ISSN: 14764687. DOI: 10.1038/s41586-018-0740-8. URL: <http://dx.doi.org/10.1038/s41586-018-0740-8>.
- Linden, David E.J. (2014). “Neurofeedback and networks of depression”. In: *Dialogues in Clinical Neuroscience* 16.1, pp. 103–112. ISSN: 12948322.
- Logothetis, Nikos K. and Brian A. Wandell (2004). “Interpreting the BOLD Signal”. In: *Annual Review of Physiology* 66.1, pp. 735–769. ISSN: 0066-4278. DOI: 10.1146/annurev.physiol.66.082602.092845.
- Maus, Bärbel et al. (2010). “Optimization of Blocked Designs in fMRI Studies”. In: *Psychometrika* 75.2, pp. 373–390. ISSN: 00333123. DOI: 10.1007/s11336-010-9159-3.

- Menon, V. (2015). “Salience Network”. In: *Brain Mapping: An Encyclopedic Reference* 2, pp. 597–611. DOI: 10.1016/B978-0-12-397025-1.00052-X.
- Moerel, Michelle, Federico De Martino, and Elia Formisano (2014). “An anatomical and functional topography of human auditory cortical areas”. In: *Frontiers in Neuroscience* 8.8 JUL, pp. 1–14. ISSN: 1662453X. DOI: 10.3389/fnins.2014.00225.
- Moradi, Afsaneh et al. (2011). “Treatment of anxiety disorder with neurofeedback: Case study”. In: *Procedia - Social and Behavioral Sciences* 30, pp. 103–107. ISSN: 18770428. DOI: 10.1016/j.sbspro.2011.10.021.
- Mottaz, Anaïs et al. (2018). “Modulating functional connectivity after stroke with neurofeedback: Effect on motor deficits in a controlled cross-over study”. In: *NeuroImage: Clinical* 20.July, pp. 336–346. ISSN: 22131582. DOI: 10.1016/j.nicl.2018.07.029.
- Nakamura, Kae, Masayuki Matsumoto, and Okihide Hikosaka (2008). “Reward-dependent modulation of neuronal activity in the primate dorsal raphe nucleus”. In: *Journal of Neuroscience* 28.20, pp. 5331–5343. ISSN: 02706474. DOI: 10.1523/JNEUROSCI.0021-08.2008.
- Nava, Elena and Brigitte Röder (2011). “Adaptation and maladaptation. Insights from brain plasticity”. In: *Progress in Brain Research* 191, pp. 177–194. ISSN: 18757855. DOI: 10.1016/B978-0-444-53752-2.00005-9.
- Niv, Sharon (2013). “Clinical efficacy and potential mechanisms of neurofeedback”. In: *Personality and Individual Differences* 54.6, pp. 676–686. ISSN: 01918869. DOI: 10.1016/j.paid.2012.11.037. URL: <http://dx.doi.org/10.1016/j.paid.2012.11.037>.
- Olds, James and Peter Milner (1954). “Positive reinforcement produced by electrical stimulation of septal area and other regions of rat brain.” In: *Journal of Comparative and Physiological Psychology* 47.6, pp. 419–427. ISSN: 0021-9940. DOI: 10.1037/h0058775. URL: <http://doi.apa.org/getdoi.cfm?doi=10.1037/h0058775>.
- Omejc, Nina et al. (2018). “Review of the therapeutic neurofeedback method using electroencephalography: EEG Neurofeedback”. In: *Bosnian Journal of Basic Medical Sciences*, pp. 213–220. ISSN: 1512-8601. DOI: 10.17305/bjbms.2018.3785.
- Paulus, Martin P. et al. (2003). “Increased activation in the right insula during risk-taking decision making is related to harm avoidance and neuroticism”. In: *NeuroImage* 19.4, pp. 1439–1448. ISSN: 10538119. DOI: 10.1016/S1053-8119(03)00251-9.

- Petersen, Steven E. and Joseph W. Dubis (2012). “The mixed block/event-related design”. In: *NeuroImage* 62.2, pp. 1177–1184. ISSN: 10538119. DOI: 10.1016/j.neuroimage.2011.09.084. URL: <https://linkinghub.elsevier.com/retrieve/pii/S1053811911011608>.
- Phillips, A. G. and H. C. Fibiger (1978). “The role of dopamine in maintaining intracranial self-stimulation in the ventral tegmentum, nucleus accumbens, and medial prefrontal cortex.” In: *Canadian journal of psychology* 32.2, pp. 58–66. ISSN: 00084255. DOI: 10.1037/h0081676.
- Ramnani, Narender and Adrian M. Owen (2004). “Anterior prefrontal cortex: Insights into function from anatomy and neuroimaging”. In: *Nature Reviews Neuroscience* 5.3, pp. 184–194. ISSN: 1471003X. DOI: 10.1038/nrn1343.
- Redgrave, Peter et al. (2010). “Goal-directed and habitual control in the basal ganglia: Implications for Parkinson’s disease”. In: *Nature Reviews Neuroscience* 11.11, pp. 760–772. ISSN: 1471003X. DOI: 10.1038/nrn2915. URL: <http://dx.doi.org/10.1038/nrn2915>.
- Rogers, Robert D. et al. (1999). “Choosing between small, likely rewards and large, unlikely rewards activates inferior and orbital prefrontal cortex”. In: *Journal of Neuroscience* 19.20, pp. 9029–9038. ISSN: 02706474.
- Ros, T. et al (2016). “Closed-loop brain training: the science of neurofeedback”. In: *Nature Reviews NeuroScience* 18.2, pp. 86–100. ISSN: 14710048. DOI: 10.1038/nrn.2016.164. URL: <https://doi.org/10.1038/nrn.2016.164>.
- Scharnowski, Frank, Chloe Hutton, et al. (2012). “Improving visual perception through neurofeedback”. In: *Journal of Neuroscience* 32.49, pp. 17830–17841. ISSN: 02706474. DOI: 10.1523/JNEUROSCI.6334-11.2012.
- Scharnowski, Frank, Ralf Veit, et al. (2015). “Manipulating motor performance and memory through real-time fMRI neurofeedback”. In: *Biological Psychology* 108, pp. 85–97. ISSN: 18736246. DOI: 10.1016/j.biopsycho.2015.03.009. URL: <http://dx.doi.org/10.1016/j.biopsycho.2015.03.009>.
- Sescousse, Guillaume, Yansong Li, and Jean Claude Dreher (2013). “A common currency for the computation of motivational values in the human striatum”. In: *Social Cognitive and Affective Neuroscience* 10.4, pp. 467–473. ISSN: 17495024. DOI: 10.1093/scan/nsu074.
- Shereena, E. A. et al. (2019). “EEG Neurofeedback Training in Children With Attention Deficit/Hyperactivity Disorder: A Cognitive and Behavioral Outcome Study”. In: *Clinical EEG and Neuroscience* 50.4, pp. 242–255. ISSN: 21695202. DOI: 10.1177/1550059418813034.



- Singh-Curry, Victoria and Masud Husain (2009). “The functional role of the inferior parietal lobe in the dorsal and ventral stream dichotomy”. In: *Neuropsychologia* 47.6, pp. 1434–1448. ISSN: 00283932. DOI: 10.1016/j.neuropsychologia.2008.11.033.
- Sitaram, Ranganatha, Sangkyun Lee, et al. (2011). “Neurofeedback and Neuromodulation Techniques and Applications”. In: Elsevier Inc. Chap. Chapter 9. Real-Time Regulation and Detection of Brain States from fMRI Signals, pp. 227–253. ISBN: 9780123822352.
- Sitaram, Ranganatha, Tomas Ros, et al. (2016). “Closed-loop brain training: The science of neurofeedback”. In: *Nature Reviews Neuroscience* 18.2, pp. 86–100. ISSN: 14710048. DOI: 10.1038/nrn.2016.164. URL: <http://dx.doi.org/10.1038/nrn.2016.164>.
- Skottnik, Leon et al. (2019). “Success and failure of controlling the fMRI-neurofeedback signal are reflected in the striatum”. In: January, pp. 1–15. ISSN: 21623279. DOI: 10.1002/brb3.1240.
- Snow, Wanda M, Brenda M Stoesz, and Judy E Anderson (2014). “The Cerebellum in Emotional Processing: Evidence from Human and Non-Human Animals”. In: June. DOI: 10.3934/Neuroscience2014.1.96.
- Sorger, Bettina, Tabea Kamp, et al. (2018). “When the Brain Takes ‘BOLD’ Steps: Real-Time fMRI Neurofeedback Can Further Enhance the Ability to Gradually Self-regulate Regional Brain Activation”. In: *Neuroscience* 378, pp. 71–88. ISSN: 18737544. DOI: 10.1016/j.neuroscience.2016.09.026. URL: <http://dx.doi.org/10.1016/j.neuroscience.2016.09.026>.
- Sorger, Bettina, Frank Scharnowski, et al. (2019). “Control freaks: Towards optimal selection of control conditions for fMRI neurofeedback studies”. In: *NeuroImage* 186.November 2018, pp. 256–265. ISSN: 10959572. DOI: 10.1016/j.neuroimage.2018.11.004. URL: <https://doi.org/10.1016/j.neuroimage.2018.11.004>.
- Sousa, Teresa et al. (2016). “Control of Brain Activity in hMT+/V5 at Three Response Levels Using fMRI-Based Neurofeedback/BCI”. In: *Plos One* 11.5, e0155961. ISSN: 1932-6203. DOI: 10.1371/journal.pone.0155961. URL: <http://dx.plos.org/10.1371/journal.pone.0155961>.
- Stalnaker, Thomas A. et al. (2018). “Orbitofrontal neurons signal reward predictions, not reward prediction errors”. In: *Neurobiology of Learning and Memory* 153, pp. 137–143. ISSN: 10959564. DOI: 10.1016/j.nlm.2018.01.013. URL: <https://doi.org/10.1016/j.nlm.2018.01.013>.

- Sulzer, J et al. (2013). “Real-time fMRI neurofeedback: progress and challenges.” In: *NeuroImage* 76, pp. 386–99. ISSN: 1095-9572. DOI: 10.1016/j.neuroimage.2013.03.033. URL: <http://www.ncbi.nlm.nih.gov/pubmed/23541800>.
- Sutton, R.S and A.G. Barto (1998). *Reinforcement learning: An introduction*. MIT Press. ISBN: 0-262-19398-1.
- TurboBrainVoyager* (n.d.). <http://www.brainvoyager.com/TurboBrainVoyager.html>. Accessed: 2019-07-30.
- Ullsperger, Markus and D. Yves Von Cramon (2003). “Error monitoring using external feedback: Specific roles of the habenular complex, the reward system, and the cingulate motor area revealed by functional magnetic resonance imaging”. In: *Journal of Neuroscience* 23.10, pp. 4308–4314. ISSN: 02706474.
- Volz, Kirsten G., Ricarda I. Schubotz, and D. Yves Von Cramon (2004). “Why am I unsure? Internal and external attributions of uncertainty dissociated by fMRI”. In: *NeuroImage* 21.3, pp. 848–857. ISSN: 10538119. DOI: 10.1016/j.neuroimage.2003.10.028.
- Walker, Jonathan E. and Gerald P. Kozlowski (2005). “Neurofeedback treatment of epilepsy”. In: *Child and Adolescent Psychiatric Clinics of North America* 14.1 SPEC.ISS. Pp. 163–176. ISSN: 10564993. DOI: 10.1016/j.chc.2004.07.009.
- Weiskopf, Nikolaus (2012). “Real-time fMRI and its application to neurofeedback.” In: *NeuroImage* 62.2, pp. 682–92. ISSN: 1095-9572. DOI: 10.1016/j.neuroimage.2011.10.009. URL: <http://www.ncbi.nlm.nih.gov/pubmed/22019880>.
- Zhang, Gaoyan et al. (2013). “Improved Working Memory Performance through Self-Regulation of Dorsal Lateral Prefrontal Cortex Activation Using Real-Time fMRI”. In: *PLoS ONE* 8.8, pp. 1–9. ISSN: 19326203. DOI: 10.1371/journal.pone.0073735.
- Zhao, Xiaojie et al. (2013). “Causal interaction following the alteration of target region activation during motor imagery training using real-time fMRI”. In: *Frontiers in Human Neuroscience* 7.DEC, pp. 1–8. ISSN: 16625161. DOI: 10.3389/fnhum.2013.00866.